Environmental Earth Sciences (2022) 81:175
https://doi.org/10.1007/s12665-022-10275-2

ORIGINAL ARTICLE

Stream sediments as a repository of U, Th and As around abandoned uranium mines in central Portugal: implications for water quality management

P. C. S. Carvalho[1,2] · I. M. H. R. Antunes[3] · M. T. D. Albuquerque[4,6] · A. C. S. Santos[1] · Pedro Proença Cunha[5]

Received: 22 November 2020 / Accepted: 5 February 2022

Abstract

This work focuses on the study of water–sediment interaction around abandoned uranium mines with open-pit lakes and mine dumps. Nineteen water and eleven stream sediment samples were collected in the abandoned Barrôco D. Frango mine, central Portugal. The trace element distribution was compared with other abandoned uranium mines in Portugal and worldwide. Generally, U, Th, and As contents in the open-pit water are high and similar to those of downstream water, suggesting its influence on aquatic systems. In abandoned mines with small to medium U exploitation, the stream sediments are moderately to heavily contaminated with U, Th and As, being U and As the most important contaminants, confirmed by their partition coefficients. A moderate to considerable potential ecological risk (34–79) was found around the abandoned Barrôco D. Frango mine area, mainly due to As contents in stream sediments. Water and stream sediments from abandoned U mines worldwide have U levels of up to 436 µg/L and 5024 mg/kg, respectively, while those from Barrôco D. Frango have 37.3 µg/L and 189 mg/kg, respectively. However, the longer the distance from the Barrôco D. Frango open-pit lake and mine dump, the higher U, Th and As contents in stream sediments, which is a warning indicator. Cluster heat maps of the water composition from four abandoned uranium mine areas show that Mondego Sul and Barrôco D. Frango mines are the most geochemically similar. Results show that stream sediments should be included in water quality management and future remediation plans of abandoned uranium mines.

Keywords Water–sediment interaction · Quality indicators · Ecological risk · Arsenic · Uranium mines

Introduction

There are about 150 uranium mines in the EU (Raeva et al. 2014), ca. 60 of which were economically exploited in the north and central mainland Portugal (between 1908 and 2001; e.g., Carvalho 2014). In central Portugal, most of the uranium mine sites are located in the uranium-bearing Beiras area; however, nowadays, most of them are closed and abandoned (Carvalho et al. 2010; Pereira et al. 2014). These mines have legacies of millions of tons of waste rock and mill tailings (World Nuclear Association 2015). Most of these mines are not remediated and some of them also have open-pit lakes.

Uranium mining activities are an important contributor to the anthropogenic flux of uranium to the environment (Sen and Peucker-Ehrenbrink 2012). Uranium mines are also often associated with the environmental release of potentially toxic elements (e.g., Costa et al. 2017; Neiva et al. 2014, 2015, 2016, 2019; Antunes et al. 2018, 2019,

✉ P. C. S. Carvalho
paulacscarvalho@gmail.com

1 GeoBioTec- GeoBioSciences, GeoTechnologies and GeoEngineering, Department of Geosciences, University of Aveiro, Aveiro, Portugal

2 MARE – Marine and Environmental Science Centre, Department of Life Sciences, University of Coimbra, Coimbra, Portugal

3 ICT, University of Minho, Braga, Portugal

4 IPCB, Instituto Politécnico de Castelo Branco, 6001-909 Castelo Branco, Portugal

5 MARE - Marine and Environmental Sciences Centre, Department of Earth Sciences, University of Coimbra, Coimbra, Portugal

6 ICT – Instituto de Ciências da Terra, Universidade de Évora, Évora, Portugal

Published online: 07 March 2022

2020, 2021) from ore, waste rocks and reagents used in the extraction process (Cuvier et al. 2016) inducing adverse influence on water, sediments and human health. The abandoned open-pit lakes associated with mine exploitation are responsible for the trace elements dispersion to streams and aquifer systems, through water–rock interaction processes (Bowell 2002).

Several studies have shown that stream sediments in abandoned uranium and radium mining areas accumulate significant higher potentially toxic elements contents (Yi et al. 2020; Zheng et al. 2020). Contaminants are preferentially stored in the suspended matter than in dissolved form, due to the affinity of trace elements for the particulate phase (Singh et al. 2005; Hsu et al. 2016; Addo-Bediako et al. 2021; Astatkie et al. 2021). Ultimately, the suspended solids can be accumulated in bottom sediments by settling and processes of water–sediment-biological components which can occur with adsorption, desorption, precipitation and biological adsorption (Wang and Li 2011). The interaction of potentially toxic elements in the interface water–sediment depends on several factors, including the physico-chemical characteristics of water (Miranda et al. 2021), mineralogy of sediments (Xie et al. 2018), cation exchange capacity and sediment grain size (Shang et al. 2011; Tansel and Rafiuddin 2016) and type of available complexing agents in water, such as carbonates, phosphates and sulfates, etc. (Silva and Nitsche 1995; Langmuir 1997). These parameters influence the chemical form of contaminants (speciation) and control their mobility, bioavailability and toxicity (Tessier and Campbell 1987). The oxidized species of uranium (U^{VI}) typically form more stable aqueous complexes and are more mobile than the reduced forms (Mühr-Ebert et al. 2019). However, potentially toxic elements present different mobility, such as reduced arsenic species that are more mobile and toxic than oxidized species (Panagiotaras and Nikolopoulos 2015).

Stream sediments have an important role in the retention of contaminants. Therefore, stream sediments are considered a good indicator for water quality, anthropogenic history of metal pollution and ecological impacts (e.g., Yan et al. 2010; Wang et al. 2018; Calmuc et al. 2021). Sediment quality and ecological indicators have been developed to assess the pollution status and ecological risk of potentially toxic elements, such as geo-accumulation index (I-geo), contamination factor (Cf) and ecological risk index (RI). An estimation of the mobility of contaminants in the streams has been also applied through the determination of partitioning coefficient, which determines the ratio of metal concentrations between solid and dissolved phases at equilibrium (Jung et al. 2005; Feng et al. 2017).

In literature, there are several studies considering the radiological effects of uranium, however, few studies on the distribution of uranium and thorium concentrations in worldwide aquatic environments are reported. This assessment is essential to understand the mobility and toxicity of contaminants in aquatic environments and allow to take measures to avoid the environmental and ecological impacts. Therefore, the main objective of this study is to understand the distribution and mobility of uranium, thorium and other potentially toxic elements concentrations, from uranium mine dumps and open-pit lakes to stream sediments, surface water and groundwater around abandoned uranium mines. The study will be developed on four main topics, considering the: (1) interaction between stream sediments and surface water; (2) dispersion of potentially toxic elements from mine dumps and open-pit lake to downstream mining area; (3) assessment of the quality and potential ecological risk of stream sediments; and (4) comparison of potentially toxic element contents from stream sediments and waters of the study area with those of other abandoned uranium mining areas from central Portugal and worldwide.

Geological setting and site description

The abandoned Barrôco D. Frango uranium mine is located close to Freixo village, in the Almeida Municipality, about 30 km north of the town of Guarda, 180 km from the city of Coimbra (Fig. 1a). Geologically, the study area belongs to the Central Iberian Zone (CIZ) of the Iberian Massif and the uranium mine is associated with Variscan uranium-bearing granites (Fig. 1b), where other abandoned uranium mines also occur (Fig. 1c). The coarse-grained porphyritic two-mica granite predominates in the area and surrounds the fine-grained two-mica granite and the very coarse-grained porphyritic two-mica granite (Fig. 1b). There are several quartz veins, basic dykes and aplitic veins trending NE–SW, which cut the coarse-grained porphyritic two-mica granite. Quartz veins also cut the very coarse-grained porphyritic two-mica granite.

The mine consists of a mineralized breccia composed of chalcedony, masses of granite, and Fe-oxides with autunite, torbernite and pitchblende. The mineralized breccia, up to 1.5 m thick, contacts with a quartz vein trending N21–46°E, 78–80°NW and cuts the very coarse-grained porphyritic two-mica granite. The host granite is altered, having secondary muscovite, hematite, and kaolinite. A clay-filled fault occurs along with the mineralized breccia and quartz vein. The average U_3O_8 grade of the mineralized structures is 0.10%, with a maximum grade of 1.31% (Junta de Energia Nuclear 1957). The mine was active for 1 year (1988–1989) and 20.8 tons of U_3O_8 were exploited by open-pit works (Parra et al. 2002). The abandoned Barrôco D. Frango uranium mine has an open-pit lake 50 m long and 10 m wide (Figs. 2 and 3a). Around the old mine, there are several agricultural areas, some of which are cultivated with potatoes

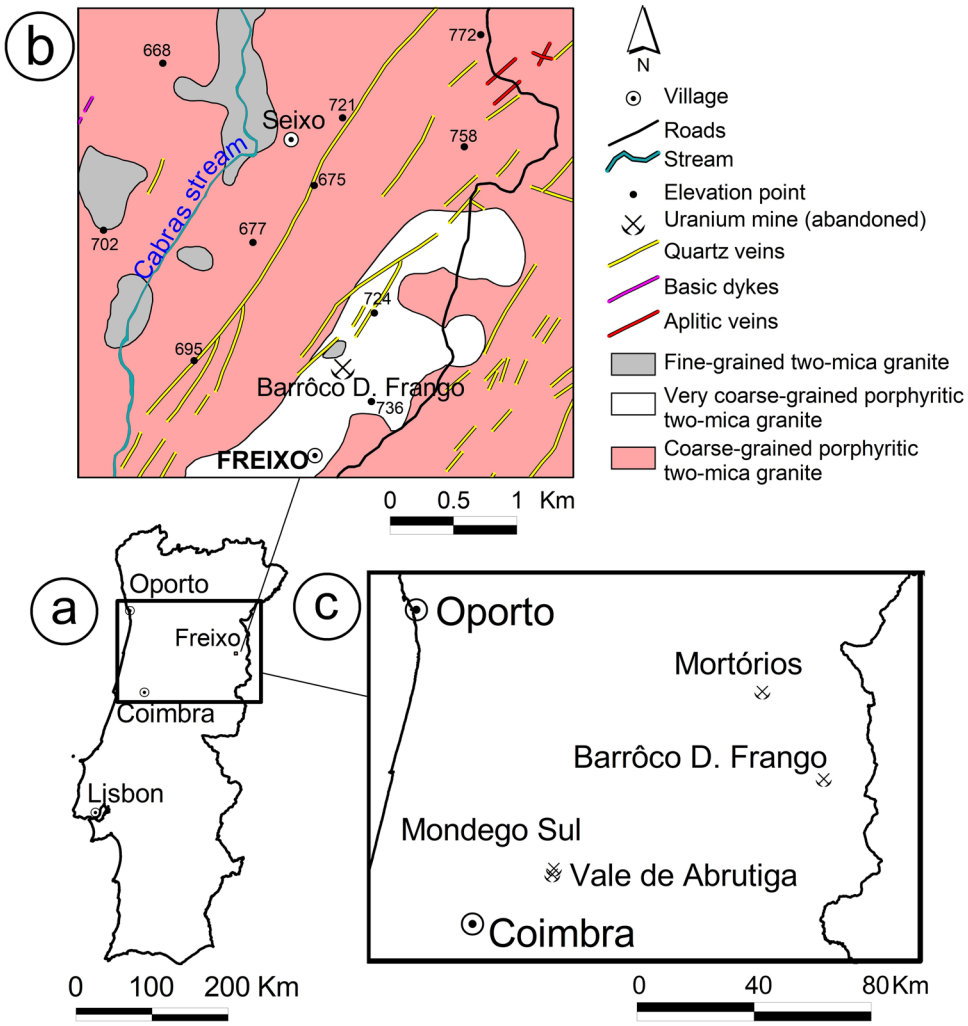

Fig. 1 Abandoned uranium mines areas: **a** Geographical location on the map of Portugal; **b** Geological map of the Barrôco D. Frango mine area (adapted from Vila Franca das Naves and Almeida Portuguese geological maps (LNEG) at the scale of 1/50000; Teixeira et al. 1959; 1962); **c** Geographical location of abandoned Mortórios, Barrôco D. Frango, Mondego Sul and Vale de Abrutiga uranium mines

and other crops, vineyards, and pastures. The water from open-pit lake is used to irrigate agricultural areas located around it (Fig. 3a, b). One dump retained the waste from the mine exploitation, composed by material with different grain sizes and uranium minerals (Fig. 3c, d) and without any compaction. The total waste volume in the area is estimated at 40,020 m^3 (European Commission 2011). The area was not remediated.

The closest village is Freixo, which is located about 500 m far from the open-pit lake and mine dump. The hydrology of the area is dominated by a first-order stream, the Cabras stream that is a tributary of the right bank of the Côa River, belonging to the Douro River Basin. The main surface water drainage directions are E-W and SE-NW towards the Cabras stream (Fig. 2). The surface drainage has a low water flux (Fig. 3b) in the summer and locally the stream dries. The mine dump and the open-pit lake are located about 2.2 km East of the Cabras stream (Cabras stream drainage basin) (Fig. 2). The mine dump is located very close to the open-pit lake (less than 100 m) (Fig. 2) and was only slightly covered by vegetation (Fig. 3c), promoting direct infiltration of water and transport of material.

The sampling campaign was done during the hydrological year of 2016/2017, in which the monthly precipitation ranged from a maximum of 80.7 mm in November 2016 to a minimum of 0.1 mm in July 2017 (SNIRH 2018). The minimum temperature reached – 3 °C during winter (December–March) and up to 40 °C during the summer (June–September).

Materials and methods

Sampling and analysis

A total of eleven stream sediment samples, located downstream of the open-pit lake and mine dump (DPL) (S1, S2, S5, S6, S7, S9, S12, S13, S14, S18 and S19) and one outside the mining influence (OMI) (S15) (Fig. 2), were collected in March 2016. Sediment composite samples were collected

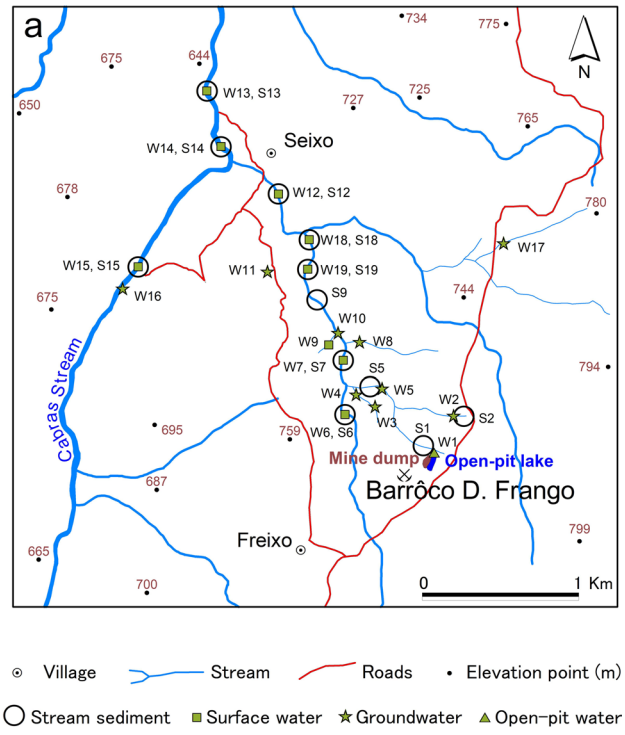

Fig. 2 The abandoned Barrôco D. Frango uranium mine study area, with the location of the mine dump, open-pit lake, stream sediment (S) and water (W) samples

up to 20 cm depth from the streambed in the middle of the channel using a scoop or a grab depending on water column depth. Then, samples were transported in polyethylene bags to the Department of Earth Sciences of the University of Coimbra (Portugal). They were dried at 40 °C, disaggregated with a silicone hammer and sieved through 2 mm and 250 µm sieves. The pH was measured in a solid–water suspension (liquid/solid ratio of 2.5) and using the British standard (British standard 1995a). The electrical conductivity (EC) was measured in a liquid/solid ratio of 1/5 and using the (British standard 1995b). The pH, EC and temperature were measured using multi-element equipment of Hanna Instruments. Stream sediment samples < 250 µm were digested with aqua regia (3:1 HCl–HNO_3), filtered through a 2 µm pore size filter and analyzed for Al, As, Co, Cr, Cu, Fe, Mn, Ni, Pb, Sr, Th, U, W and Zn by Inductively Coupled Plasma Optical Emission Spectroscopy (ICP-OES of Horiba Jovin Yvon, model YV20002 spectrometer with a monochromator). An in-house soil was prepared with aqua regia and analyzed and validated using the certified sewage sludge amended soil BCR-143 R. A laboratory standard and duplicate blanks were analyzed at the beginning and the end of determinations of the stream sediment samples. The precision of determinations was better than 4%. The detection limits were converted from mg/kg by estimation using the equation (DL /mg/kg) = (X*0.1)/m, where X is the DL at (mg/L) given by the ICP-OES analysis and m is the average of heavy masses of the samples in kg. The detection limits are presented in Appendix A.

Five stream sediment samples (S1, S6, S12, S13, S14) containing the highest and one (S15) the lowest U and Th concentrations were selected to obtain the percentages of gravel (> 2 mm), sand (2 mm–63 µm), silt (63–4 µm) and clay (< 4 µm), through the combination of two methods: sieving the fraction > 63 µm and by laser diffraction analysis of the fraction < 63 µm with a Coulter laser granulometer (2 mm–0.04 µm; precision up to 2%). A Philips PW3710 X-ray diffractometer, with a Cu tube, at 40 kV and 80 nA, was used to obtain the mineralogical composition of the < 2 µm fraction in oriented samples before and after heating to 550 °C, but also with an ethylene glycol treatment. These determinations were carried out in the Sedimentology Laboratory of the Department of Earth Sciences, University of Coimbra.

The organic matter (OM) and cation exchange capacity (CEC) were determined in the selected stream sediment samples. An elemental analyser (SC 144 DR, LECO) was used to determine the organic carbon (OC) by combustion. The samples were heated at 590 °C, oxidized to CO_2 and quantified in the infra-red gas cell. The Van Bemmelon factor of 1.724 (Tabatabai 1996) was used to quantify the organic matter (% OM = %OC × 1.724), with an accuracy of 1%. The CEC, in cmol/kg, was determined with 1 M ammonium acetate pH 7 (1/10) extraction (Thomas 1982) followed by atomic absorption spectrometry (PinAAcle 900 T, Perkin Elmer). At pH 7.0, the CEC was calculated from the individual cation values (sum of exchangeable bases + exchange acidity). The exchange acidity was obtained by extraction with 1 N potassium chloride (1/20) and titration with NaOH at pH = 7.0 (Chernov 1947; Nye et al. 1961) with an accuracy of 0.38%. These determinations were carried out in the Soil and Fertility Laboratory of the Agrarian School of Coimbra (Portugal).

A total of 19 water sampling points (1 open-pit lake—W1; 6 wells—W16, W4, W5, W8, W10; W11, 3 springs—W17, W2, W3 and 9 streams—W15, W6, W7, W9, W12, W13, W14, W18, W19; Fig. 2) were collected four times in the hydrological year, in March, July and November 2016 and January 2017, respectively. A total of 72 water samples were analyzed for F^-, Cl^-, NO_2^-, SO_4^{2-}, NO_3^-, PO_4^{3-}, HCO_3^-, Na, K, Ca, Mg, Al, B, Ba, Cd, Co, Cr, Cu, Fe, Li, Mn, Ni, Pb, Sr, Zn, As, Th and U. Four streams were dry during the sampling (W6, W9, W12 and W18) and one spring (W3); thus, a total of six samples were not sampled (July and November 2016). The water samples from the stream (W15), well (W16) and spring (W17) are located at the OMI (Fig. 2; Appendix A).

The pH, oxidation–reduction potential (ORP), electrical conductivity (EC), temperature and dissolved oxygen

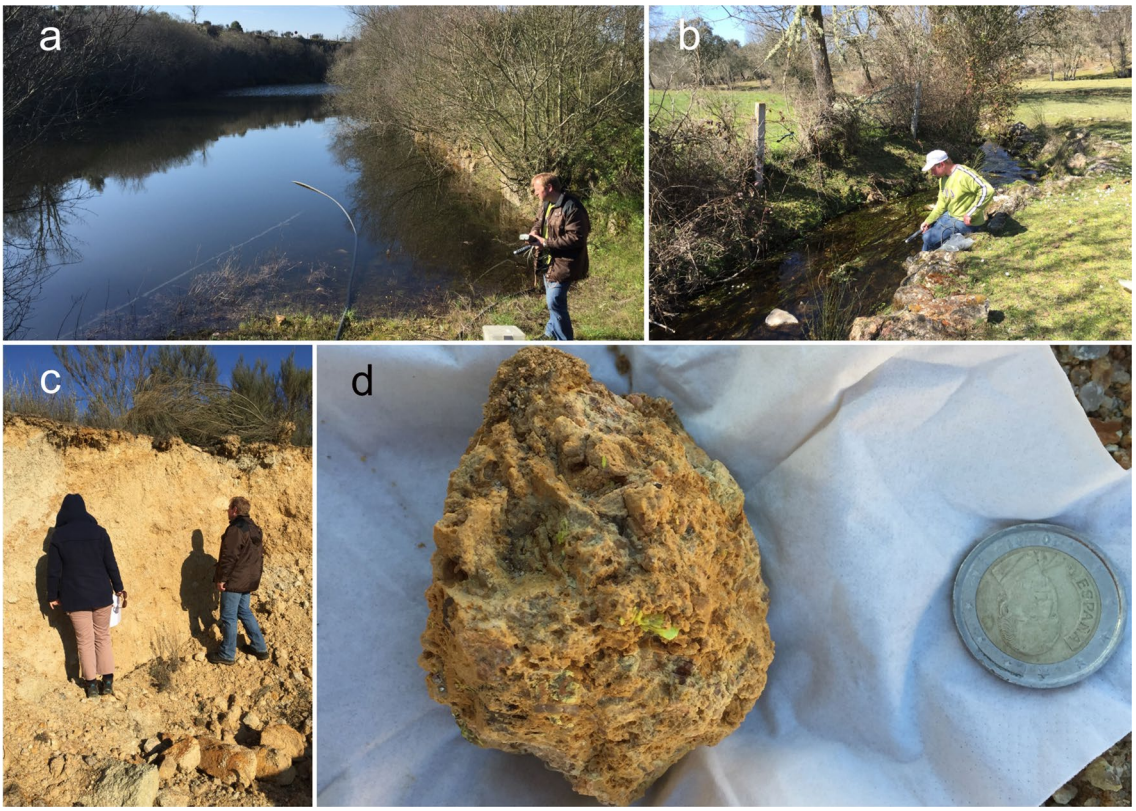

Fig. 3 Selected photographs of the sampling campaign in March 2016: **a** W1 sample site (for location see Fig. 2), located in the NNE margin of the open-pit lake; **b** collecting the water sample W13 from the Cabras stream, the most downstream sample site from the study area, also showing the surrounding agricultural areas; **c** an exposure of the mine dump; **d** observed uranium minerals (e.g., autunite) in the mine waste materials (the coin´s diameter is 25.75 mm)

(DO) were measured in situ with Hanna Instruments Model HI9829. The Eh corresponds to the ORP result + 209 according to the Ag:AgCl electrode used as a reference for the assumed T = 15 °C (Nordstrom and Wilde 2005). The alkalinity (HCO_3^-) was measured according to the method of Brown et al. (1970). Due to the small size of the stream sampled, waters were collected below the water surface, trying to move the bottle up and down to sample the entire vertical column of water avoiding sediments that could modify the water composition. Groundwater samples were collected from pumping wells after several hours of pumping before sampling to remove groundwater stored in the well and rainwater. Afterward, groundwater was collected at about 1 m below the surface using a grab sampler. The water samples were transported in polypropylene bottles within cooler boxes to the Department of Earth Sciences—University of Coimbra. The samples were filtered through 0.45 µm pore size cellulose acetate membrane filters. Anions were determined in non-acidified samples by chromatography with a Dionex ICS 3000 Model. The samples for the determination of cations were acidified with HNO_3 to pH 2 and analyzed by an ICP-OES at the same Department. Duplicate blanks and a laboratory water standard were analyzed for quality control. The precision was better than 5%. The detection limits of elements analyzed in waters are given in Appendix A. The total dissolved solids (TDS) and total solids (TS) were determined after evaporation of 100 mL of filtered and unfiltered water through 0.45 µm filters, respectively. Ion balance errors are better than 10%.

Speciation modeling

The speciation modeling was carried out using the PhreeqC 3.1.5 software and sit database (Parkhurst and Appelo 1999). The alkaline earth elements reactions and log K values were added to the PhreeqC input file (Dong and Brooks 2006; Geipel et al. 2008) for the uranium modeling, as follows,

$2Ca^{2+} + UO_2^{2+} + 3CO_3^{2-} = Ca_2UO_2(CO_3)_3$; log K = 30.79.

$Ca^{2+} + UO_2^{2+} + 3CO_3^{2-} = CaU(CO_3)_3^{2-}$; log K = 27.18.

$Mg^{2+} + UO_2^{2+} + 3CO_3^{2-} = MgUO_2CO_3^{2-}$; log K = 26.11.

$Sr^{2+} + UO_2^{2+} + 3CO_3^{2-} = Sr\,UO_2\,(CO)_3^{2-}$; log K = 26.86.

$2Sr^{2+} + UO_2^{2+} + 3CO_3^{2-} = Sr_2UO_2(CO)_3$; log K = 29.73.

The saturation index (SI) is an indicator that identifies the saturation status of minerals in the water. When SI = 0, the minerals in the aqueous solutions are in equilibrium,

when SI < 0, the minerals in the aqueous solutions have not reached saturation and remain in solution. When SI > 0, an oversaturation of water by the given mineral is reached and mineral precipitation will occur. The SI was determined using PhreeqC and is defined as follows (1),

$$SI = log\frac{IAP}{K_{eq}}, \tag{1}$$

where IAP is the ion activity product and K_{eq} is the equilibrium constant of mineral dissolution at a chosen temperature.

Interaction between stream sediments and water

The partition coefficient (K_d kg L^{-1}) is the ratio between a pollutant concentration in sediment C_s(mg Kg^{-1}) and its concentration in water C_w(mg L^{-1}), in a balanced water–sediment system. The partition coefficient is, thus, a useful parameter to determine the behavior of potentially toxic elements in a water environment and reflects the potential ecohazard and migration of pollutants between water phase and solid phase.

The $logK_d$ of the stream sediments/waters from Barrôco D. Frango were compared with those from USEPA (2005) and IAEA (2010).

Contamination indexes

Geo-accumulation index

The geo-accumulation index (I_{geo}) was proposed by Müller (1979) and is an evaluation method used to quantify the degree of metal accumulation in soils and sediments. It is calculated as follows:

$$\mathrm{I}_{\mathrm{geo}=\log_2\left(\frac{\mathrm{C_n}}{1.5\times \mathrm{B_n}}\right)}, \tag{2}$$

where C_n is the element concentration in the sediment, and B_n is the background concentration of the element. In this study, the background concentration of the element is the median determined by Ferreira (2000). Factor 1.5 is used to minimize the effect of variations in the background values, which can be due to lithogenic variations or local anthropogenic effects. The classes of I_{geo} are presented in Table 1.

Potential ecological risk

The potential ecological risk index (RI) was proposed by Håkanson (1980) to use sediments as a diagnostic tool for aquatic pollution control purposes, by assessing the potential ecological risk considering both the toxicity and the response factor of metals. This index is computed in three different phases; in the first phase the contamination factor (C_f), in the second phase the potential ecological risk factor (E_R) is determined and finally, the potential ecological risk index (RI) can be calculated as follows (3, 4, 5):

$$C_f^i = \frac{C_D^i}{C_R^i}, \tag{3}$$

$$E_R^i = \frac{T_R^i}{C_f^i}, \tag{4}$$

$$RI = \sum_{i-1}^{m} E_R^i, \tag{5}$$

where C_D^i is the element concentration in each sample; C_R^i is the background value, in this study is the median values (Ferreira 2000); T_R^i is the biological toxic factor for each element, which are As = 10, Cr = 2, Cu = Pb = Ni = 5, Zn = 1, according to Håkanson (1980). The full method to determine the ecological risk index includes eight pollutants, however, in this study PCBs, Hg and Cd were not considered, and classes were readjusted. Therefore, the maximum value of T_R^i (As = 10) was considered as the lowest level limit of E_R^i and the remaining classes followed by doubles, which means that the concentrations of elements within a water system are compared with a reference system that has no contamination ($C_f^i = 1$) (Håkanson 1980). The same procedure was used for the first level of RI, which will be the sum of T_R^i values of all elements, which is 28 in this study, thus the threshold for RI can be 30. Therefore, the readjusted E_R^i and RI classes are presented in Table 1.

Statistical methodologies

The water samples composition from the abandoned Barrôco D. Frango uranium mine area was compared with those of three selected old Portuguese uranium mines, Vale de Abrutiga, Mondego Sul and Mortórios, through the construction of cluster heat maps (Wilkinson and Friendly 2009), aiming to establish regional geochemical spatial distribution patterns for the stream sediments and waters. A cluster heat map is a graphical display that reveals together row and column hierarchical cluster structure, within a data matrix. It consists of a rectangular tiling, with each tile shaded on a color scale representing the value intensity of the corresponding element. The rows and columns of the tiling are ordered such that the most similar stand near each other. On the vertical and horizontal margins of the tiling are hierarchical cluster trees simultaneously revealing row and column's hierarchical clustering (Wilkinson and Friendly 2009; Cerdas et al. 2017). Indeed, exploring features/individual matrices to examine how correlated features

Table 1 Classes of Igeo and adjusted classes of potential ecological risk of potentially toxic elements in stream sediments from Barrôco D. Frango

Correspondence between Igeo values and Igeo classes according to Müller (1979, 1981)		
Igeo	Igeo classes	Sediment quality
< 0	0	practically uncontaminated
> 0–1	1	uncontaminated to moderately contaminated
> 1–2	2	moderately contaminated
> 2–3	3	moderately to heavily contaminated
> 3–4	4	heavily contaminated
> 4–5	5	heavily to extremely contaminated
> 5	6	extremely contaminated
Threshold*	Modified threshold	Degree of risk
$C_f^i < 1$	–	Low
$1 \leq C_f^i < 3$	–	Moderate
$3 \leq C_f^i < 6$	–	Considerable
$C_f^i \geq 6$	–	Very high
$C_d < 8$	$C_d < 5$	Low
$8 \leq C_d < 16$	$5 \leq C_d < 10$	Moderate
$16 \leq C_d < 32$	$10 \leq C_d < 20$	Considerable
$C_d \geq 32$	$C_d \geq 20$	Very high
$E_R^i < 40$	$E_R^i < 10$	Low
$40 \leq E_R^i < 80$	$10 \leq E_R^i < 20$	Moderate
$80 \leq E_R^i < 160$	$20 \leq E_R^i < 40$	Considerable
$160 \leq E_R^i < 320$	$40 \leq E_R^i < 80$	High
$E_R^i \geq 320$	$E_R^i \geq 80$	Very high
RI < 150	RI < 30	Low
$150 \leq RI < 300$	$30 \leq RI < 60$	Moderate
$300 \leq RI < 600$	$60 \leq RI < 120$	Considerable
RI ≥ 600	RI ≥ 120	Very high

*According to Håkanson 1980

correspond to similar individuals is a powerful classification tool. Both features and individuals are clustered independently using ascendant hierarchical clustering based on Euclidian distances. A heat map is then displayed, reflecting data in the permuted matrix where the data values are replaced by corresponding color intensities.

Results and discussion

Geochemistry of waters

Physico-chemical parameters and chemical results of water samples from the abandoned Barrôco D. Frango uranium mine area are given in Appendix A. According to the Piper classification (Piper 1944), most water samples are bicarbonate (HCO_3) and mainly of sodium–potassium type, but some of them are also of an undefined type and rarely calcium type.

The pH values of waters from open-pit lake range from 6.23 to 6.86. On the water group OMI, the pH values of springs range from 4.97 to 6.24 and those of streams range from 6.48 to 7.54. On the water group DPL, pH values of springs range from 5.64 to 6.73, wells from 5.31 to 7.39 and streams from 5.83 to 7.55 (Appendix A). These results are consistent with those reported in the literature (e.g., Gómez et al. 2006). The water samples present Eh values varying from 323 to 602 mV and EC ranging between 13 and 172 µS/cm, without any differences between water samples collected at the OMI and the DPL (Appendix A).

In general, the waters from the open-pit lake do not show concentrations of U and Th significantly different from those of surface waters from DPL (Appendix A, Fig. 4). However, the open-pit lake presents high Fe and Mn concentrations, suggesting the occurrence of high metal contents. Fe and Mn contents could have precipitated as oxy-hydroxides in the open-pit lake, due to the pH that ranges from 6.23 to 6.86, as postulated by Eary (1999). These oxy- hydroxides could

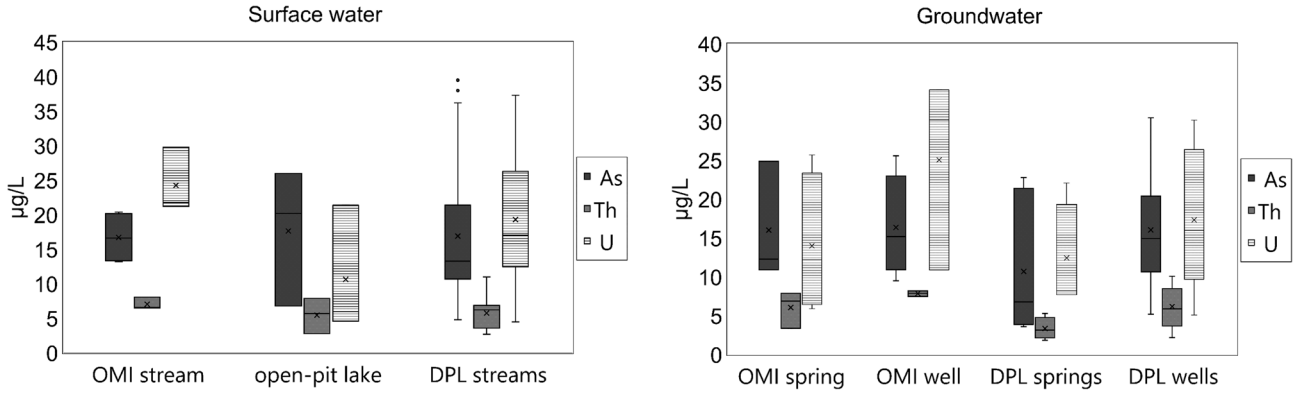

Fig. 4 Box–Whisker plots showing the variability of As, Th and U in surface waters and groundwaters from the abandoned Barrôco D. Frango uranium mine area. OMI—outside the mining influence; DPL—downstream of the open-pit lake and mine dump

have flocculated with concomitant adsorption of the metals that would have deposited in the deeper layers of the open-pit. The Eh values of water from the open-pit lake range from 374 to 540 mV. The adsorbed metals and uranium may eventually enter the solution with a decrease of oxidation–reduction potential and/or pH value. In the campaigns carried out in the open-pit lake, there was a decrease in Eh, but the pH remained almost constant, and thus the speciation of the potentially toxic elements would have remained constant as well (Fig. 5a, b; Appendix A). The water from the open-pit has been used for the irrigation of pasture (EDM 2017), which increases the dispersion potential of U and As and probable entrance into the food chain.

The average Na, K, Ca and Mg contents are higher in DPL surface and groundwater than in OMI water. Moreover, average Al, B, Ba, Co, Cu, Li, Mn, Ni, Sr and As contents are higher in DPL surface water, while average Al, B, Cu, Li, Sr and Zn contents are higher in DPL groundwaters than in OMI waters. There is an attenuation in U and Th contents in DPL surface and groundwaters that might be caused by adsorption in oxi-hydroxides precipitated in the streams and in the groundwater.

The highest U contents in stream water and groundwater occurred in the winter (January 2017; Appendix A) with the highest water flow and leaching from the dump to downstream water as reported in other studies (Neiva et al. 2014, 2016, 2019; Devaraj et al. 2021). Moreover, the bicarbonate released by weathering processes could also affect the carbonate species of U that inhibit the U sorption to aquifer systems and stream sediments (His and Langmuir, 1985). In the open-pit lake, the highest U concentration was reached in autumn (November 2016). As reported by other studies, the seasonal U variation in water from lakes is caused mainly by pH variation, biological activity and internal chemical reactions (e.g., Mochizuki et al. 2016). Some studies reported peak concentrations in summer (Mochizuki et al. 2016), while others describe high U concentration in water from lakes during the autumn and winter seasons (Kubiak and Machula 2014). In the Barrôco D. Frango open-pit lake, the U dissolved species increase during the autumn due to the increase of HCO_3^- concentration and the slight increase of Ca concentration that promotes the occurrence of U in the solution (Appendix A).

Water geochemical modeling

Speciation modeling was carried at the OMI and DPL surface water and groundwater to assess the predominant species formed by the influence of open-pit lake and mine dumps (Table 2). The arsenic occurs as pentavalent species, however, in surface water samples the $H(AsO_4)_2^-$ (up to 84.8%) occurs predominantly at the OMI, whereas $H_2(AsO_4)^-$ (up to 88.1%) occurs predominantly in DPL surface waters. These results are consistent with the Eh–pH projection for the system As–Fe–O–H–S (Fig. 5a). At the OMI and DPL groundwater samples, there are slight differences between the As species in the summer (July 2016) and winter (January 2017) sampling periods (Table 2). Cadmium, Cr, Mn and Ni occur as divalent species and there is no obvious variation in the species formed OMI and DPL (Table 2). Chromium mainly occurs as $Cr(OH)_3$ (up to 95.3%), and $Cr(OH)_2^+$ (up to 27.9%), being the most toxic form of chromium. Lead mainly occurs as a divalent form (54.7—89.2%) that raise the mobility and bioavailability of this metal. However, there is a tendency to form $PbCO_3$ species (up to 40.4% in sample W7) in DPL waters, due to the near-neutral pH (6.65) and HCO_3^- concentration in water. Iron mainly occurs as $FeCO_3OH$ showing evidence of the precipitation in these waters.

Uranium occurs as hexavalent species (Fig. 5b), accounting for the significant uranium concentrations observed in DPL water samples (W7 and W3), mainly due to its mobility. Thorium and U mainly occur in water as CO_3 complexes. The dissolution of uranium minerals with concomitant

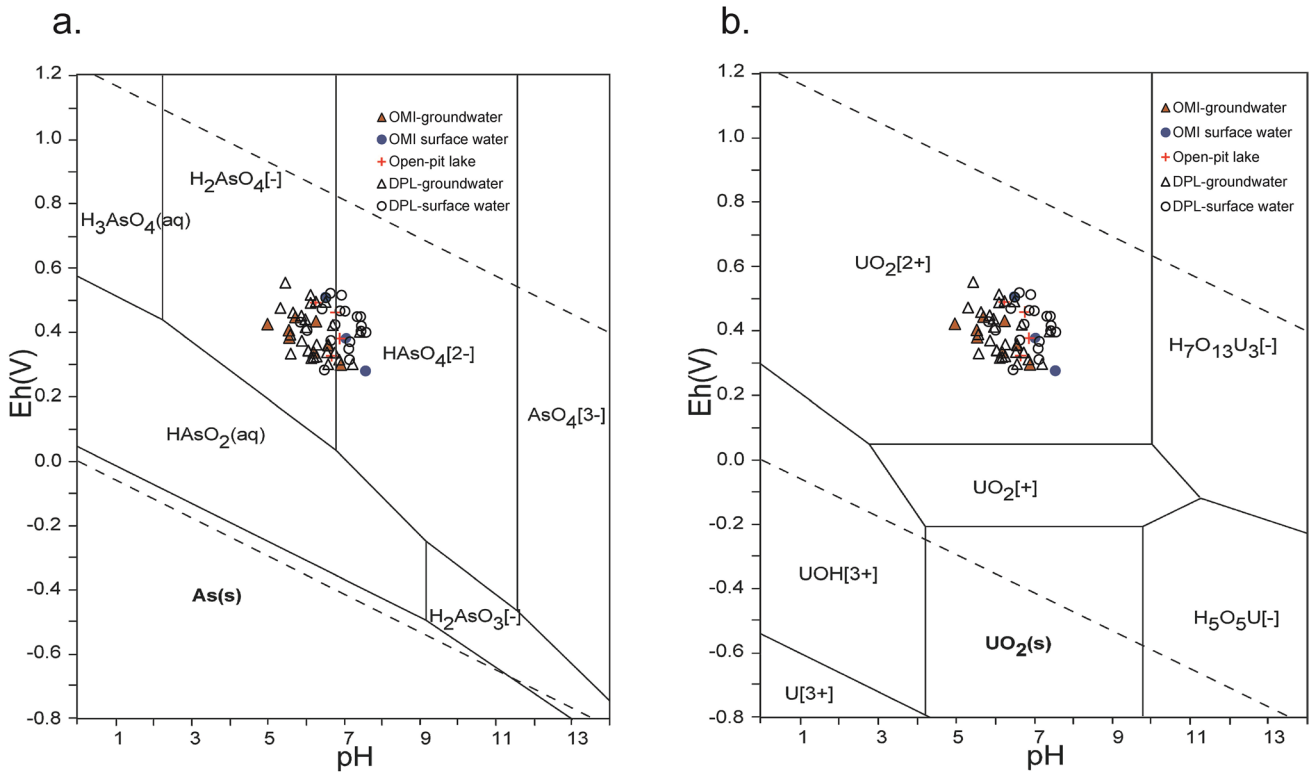

Fig. 5 Eh–pH values for the systems **a** As–O–H, **b** U–O–H of the waters from the abandoned Barrôco D. Frango uranium mine area (Adapted from Takeno 2005). OMI—outside the mining influence; DPL—downstream of the open-pit lake and mine dump

oxidation of U(IV) to U(VI) and the formation of strong complexes with anions, increase the uranium mobility (Langmuir 1978).

Thorium mainly occurs as $Th(OH)_3(CO_3)^-$ (up to 90.1%), $Th(OH)_2(CO_3)_2^{2-}$ (up to 4.5%), $Th(OH)_2(CO_3)$ (up to 45.4%) and $Th(OH)_3^+$ (up to 9.7%). Uranium mainly occurs as UO_2CO_3 (up to 89.9%), $CaUO_2(CO_3)_3^{2-}$ (up to 16.1%), $(UO_2)_2(CO_3)(OH)_3^-$ (up to 46.7%), $UO_2(CO_3)_2^{2-}$ (up to 46.7%). The HCO_3^- water concentration contributes to the formation of these carbonate complexes. Moreover, the formation of uranyl-calcium-carbonate complexes (in surface waters W15 and W7, in January 2017), which is related to Ca lixiviation by the rain waters reduces the adsorption of U(VI) (Stewart et al. 2010). Further studies are required to assess the parameters involved in the adsorption of uranyl and thorium complex to stream sediments, such as the competition for available adsorption sites and hydrochemical conditions.

A significant percentage of uncharged thorium and uranium complexes (up to 45.4% and up to 89.9%, respectively) occurs in the water, while the negative charge complex constitutes the dominant complexes thorium and uranium complexes. These carbonate complexes are a result of the pH and Eh values (5.83—7.54; 327—564 mV) and carbonate concentration. The type and charge of complexes are important to understand the adsorption processes and if required, to select more efficient remediation processes. In oxygenated waters, the formation of these stable complexes of uranium enhances its dispersion to the environment (Langmuir 1978; Markich 2002). Some water samples (W15, W17, W7 and W3) show a saturation index higher than 1, suggesting the formation of ferrihydrite, goethite, hematite, lepidocrocite. The affinity of dissolved U and Th to Fe-oxide minerals, such as hematite and goethite over a wide range of pH conditions is well known (Hsi and Langmuir 1985; Moyes et al. 2000), retarding their dispersion in the environment. The minerals in the open-pit and the groundwater sample, W10, have the same precipitation or dissolution trend in the summer and winter periods (Table 3), suggesting that this groundwater sample may have evolved from the open-pit lake.

Geochemistry of stream sediments

The textural and mineralogical characteristics, physical–chemical parameters, the potentially toxic element contents in stream sediments from the abandoned Barrôco D. Frango uranium mine area are presented in Table 4. The sand fraction dominates in all stream sediment samples. Quartz, K-feldspar and plagioclase, with accessory biotite and muscovite and, rarely, some detrital grains of iron

Table 2 Principal aqueous chemical forms of potentially toxic elements in surface waters and groundwaters close to the old Barrôco D. Frango mine predicted by PhreeqC V3.1.5 (Parkhurst and Appelo 1999)

	Outside the mining influence				Open-pit lake		Downstream of the open-pit lake and dump					
	Stream		Spring				Well		Stream		Spring	
Species names (%)	W15- July 2016	W15-Jan. 2017	W17-July 2016	W17-Jan. 2017	W1- July 2016	W1 -Jan. 2017	W10-July 2016	W10-Jan. 2017	W7-July 2016	W7-Jan. 2017	W3-July 2016	W3-Jan. 2017
$H(AsO_4)^{2-}$	64.62	84.79	23.98	20.38	–	43.26	14.39	21.33	11.09	43.97	18.63	18.25
$H_2(AsO_4)^-$	34.24	14.52	75.78	79.32	–	56.07	85.11	77.98	88.05	54.89	81.04	81.36
$Ca(HAsO_4)$	0.96	0.53	0.13	–	–	0.53	–	–	–	0.88	–	–
Cd^{2+}	96.26	96.41	98.13	98.41	95.52	96.09	93.48	90.45	96.82	94.4	97.91	–
$CdCl^+$	–	1.57	0.52	0.59	-	0.90	–	3.55	1.89	2.64	0.4	–
$CdCO_3$	0.98	1.2	–	–	0.77	–	–	–	–	–	–	–
$Cd(HCO_3)^+$	1.36	–	0.83	–	1.46	1.28	1.52	1.01	0.78	1.02	1.25	–
$CdHPO_4$	–	–	–	–	1.03	–	3.46	3.98	-	-	–	–
$Cr(OH)^{2+}$	–	–	2.8	18.25	3.09	4.61	7.60	9.35	25.79	4.12	4.17	24.56
$Cr(OH)_2^+$	3.4	3.12	14.04	24.69	-	12.69	9.56	7.17	27.86	13.75	12.99	25.63
Cr(OH)CO3	0.96	2.92	1.63	13.36	95.96	29.35	7.28	10.09	7.82	18.25	2.89	14.04
$Cr(OH)_3$	95.29	93.27	81.45	43.42	-	48.08	15.36	16.47	38.16	62.89	47.97	35.36
$Cr(HPO_4)^+$	–	–	–	–	–	–	59.18	54.67	-	-	–	–
Fe^{2+}	–	–	–	0.73	–	–	–	99.27	–	–	–	–
$FeCO_3OH$	99.75	99.82	99.68	99.16	99.59	99.90	99.92	–	99.82	–	99.89	–
Mn^{2+}	58.87	52.32	92.79	95.12	62.95	75.24	90.43	99.05	96.8	79.87	89.3	94.83
MnF2	1.76	1.09	–	–	4.50	3.47	1.77	1.45	–	1.38	3.28	1.98
$Mn(CO_3)$	38.65	46.29	6.21	3.68	31.67	20.28	6.18	6.81	2.37	17.32	6.5	2.66
Ni^{2+}	97.91	98.56	98.86	99.12	97.97	–	–	–	–	97.32	–	–
$NiHCO_3^+$	1.1	0.44	0.66	0.44	1.19	–	–	–	–	0.84	–	–
$NiSO_4$	0.42	–	0.39	0.37	0.30	–	–	–	–	1.55	–	–
Pb^{2+}	–	–	–	86.39	–	50.57	–	1.66	–	54.71	–	89.24
$PbSO_4$	–	–	–	0.92	–	0.92	–	76.57	–	2.5	–	0.91
$PbOH^+$	–	–	–	1.14	–	1.38	–	0.98	–	1.79	–	0.91
$PbCO_3$	–	–	–	11.3	–	46.90	–	19.53	–	40.36	–	8.51
$Th(OH)_3(CO_3)^-$	–	90.04	–	41.85	–	69.07	–	44.89	–	68.38	–	38.77
$Th(OH)_2(CO_3)_2^{2-}$	–	2.78	–	1.26	–	5.35	–	3.03	–	4.52	–	0.99
$Th(OH)_2(CO_3)$	–	4.0	–	42.79	–	23.64	–	44.67	–	23.22	–	45.39
$Th(OH)_3^+$	–	0.43	–	9.7	–	–	–	5.15	–	2	–	9.52
$Th(OH)_2^{2+}$	–	–	–	1.05	–	–	–	-	–	–	–	1.29
$Th(OH)_4$	–	2.74	–	3.14	–	–		1.65	–	1.77	–	2.53
UO_2CO_3	–	12.86	83.3	86.45	–	54.14	–	76.35	89.9	49.68	–	87.48
$CaUO_2(CO_3)_3^{2-}$	–	16.11	–	–	–	14.39	–	2.27	-	14.48	–	–
$(UO_2)_2(CO_3)(OH)_3^-$	–	46.67	–	4.62	–	1.27		1.18	0.85	7.17	–	3.78
$UO_2(CO_3)_2^{2-}$	–	14.35	9.88	4.44	–	19.67	–	9.06	3.95	16.36	–	–
$Ca_2UO_2(CO_3)_3$	–	3.4	–	–	–	6.05	–	1.23	-	9.2	–	–
UO_2OH^+	–	–	3.92	2.75	–	–	–	1.19	2.96	–	–	3.07

Table 2 (continued)

	Outside the mining influence				Open-pit lake		Downstream of the open-pit lake and dump					
	Stream		Spring				Well		Stream		Spring	
Species names (%)	W15- July 2016	W15-Jan. 2017	W17-July 2016	W17-Jan. 2017	W1- July 2016	W1 -Jan. 2017	W10-July 2016	W10-Jan. 2017	W7-July 2016	W7-Jan. 2017	W3-July 2016	W3-Jan. 2017
$UO_2(CO_3)_2^{2-}$	–	–	–	–	–	–	–	9.06	–	–	–	3.24
UO_2^{2+}	–	–	–	0.91	–	–	–	–	1.41	–	–	1.28
$UO_2(CO_3)(OH)_3^-$	–	–	0.99	–	–	–	–	1.18	–	–	–	
$UO_2(CO_3)_3^{4-}$	–	5.27	–	–	–	2.55	–	–	–	1.56	–	

Jan. january,– not detected

oxy-hydroxides and shales were identified in stream sediments, in macroscopic observation and under the binocular microscope (× 50). The amounts of silt and clay fractions are < 8.8% and < 0.9%, respectively. The clay minerals are illite (29–53%), kaolinite (25–40%), smectite (0–31%) and vermiculite (0.3%). Stream sediments from DPL have similar textural characteristics, pH, EC and CEC values as the OMI stream sediments (Table 4). The organic matter in DPL stream sediments is lower than 0.96% and in OMI stream sediment is 2.8%. DPL stream sediments have higher As (up to 60.6 mg/kg), Th (up to 81.9 mg/kg) and U (up to 189 mg/kg) concentrations and, generally, higher Co, Mn and Zn concentrations than the OMI stream sediment (Table 4, Fig. 6). Erosion and leaching of the mine dump and processes removing these elements from tailings and rocks are responsible for their highest concentrations in DPL stream sediments. The U is generally more abundant than Th due to autunite, torbernite and pitchblende from the breccia.

Water–sediment interaction

Stream sediments show an increase in U and Th contents with the increased distance from the open-pit lake, while waters present a slight decrease in average U and Th contents (Fig. 6). The partition coefficient logarithm ($logK_d$) between DPL stream sediments and water range from 3.61 to 4.07 for Th and from 3.21 to 4.14 for U (Table 5). The mean $logK_d$ value of Th is lower than the mean indicated by IAEA (2010) (Table 5), which suggests that Th may have more affinity to be in solution, indicating that the ecological risk in the Barrôco D. Frango area is relatively significant. The increase of uncharged Th complexes from upstream to downstream (Table 2) may justify the tendency of Th to be released into solution (Fig. 6). However, an increase in Th concentration is observed in stream sediments from upstream to downstream (Fig. 6), probably due to the occurrence of negative Th charge complexes with a great affinity to be adsorbed by organic matter (Mortvedt 1994; Wang et al. 2017) and Fe oxy-hydroxides (e.g., Barnett et al. 2000).

Otherwise, the $logK_d$ values of U tends to be higher than those reported by IAEA (2010). This is consistent with the decrease in average U contents in the DPL water samples over a kilometer, due to the adsorption by stream sediments (Fig. 6). Within a pH range of 5.15—7.23 (Table 4), U (VI) occurs mainly in hydrolyzed forms (Cowart and Burnett 1994; Barnett et al. 2000). Therefore, in slightly acidic and near-neutral conditions, U complexes are adsorbed in Fe mineral surfaces (e.g., Bargar et al. 2000; Barnett et al. 2000; Cheng et al. 2007; Zielinski et al. 2008; Gavrilescu et al. 2009; Li and Kaplan 2012; Tserenpil et al. 2013). The clay percentage (< 4 µm) of the stream sediments is low (Table 4), but clay minerals significantly adsorb U (e.g., Missana et al. 2004; Bachmaf and Merkel 2011), as well as

Table 3 Saturation index (SI) of minerals in the open-pit water and groundwater from Barrôco D. Frango

Phase	Composition	Summer (July 2016)		Winter (January 2017)	
		W1	W10	W1	W10
Anhydrite	$CaSO_4$	− 4.33	− 3.99	− 3.88	− 3.64
Aragonite	$CaCO_3$	− 2.83	− 3.35	− 2.8	− 3.18
Azurite	$Cu_3(OH)_2(CO_3)_2$	3.59	0.5	–	–
Autunite	$Ca(UO_2)_2(PO_4)_2$	–	–	− 11.18	− 12.1
Calcite	$CaCO_3$	− 2.69	− 3.2	− 2.64	− 3.03
Cuprite	Cu_2O	− 2.59	− 4.86	–	–
Dolomite	$CaMg(CO_3)_2$	− 5.44	− 6.84	− 5.78	− 6.5
Ferrihydrite	$Fe(OH)_3$	2.05	0.02	1.74	− 0.66
Goethite	FeOOH	6.55	4.04	5.39	3.16
Gypsum	$CaSO_4$:2H2O	− 4.39	− 3.91	− 3.71	− 3.51
Halite	NaCl	− 9.18	− 8.96	− 9.27	− 8.37
Hematite	Fe_2O_3	18.11	13.04	15.69	11.25
Hydroxyapatite	$Ca_5(PO_4)_3OH$	− 6.42	− 7.43	− 7.22	− 5.93
Jarosite-H	$(H_3O)Fe_3(SO_4)_2(OH)_6$	− 3.75	− -7.7	− 6.26	− 10.78
Jarosite-K	$KFe_3(SO_4)_2(OH)_6$	1.08	− 2.69	− 0.42	− 5.34
Jarosite-Na	$NaFe_3(SO_4)_2(OH)_6$	− 1.54	− 5.6	− 3.25	− 8.21
Lepidocrocite	FeOOH	5.57	3.54	5.26	2.86
Magnesite	$MgCO_3$	− 3.24	− 4.13	− 3.61	− 3.95
Magnetite	Fe_3O_4	16.32	9.19	14.14	7.95
Rhodochrosite	$MnCO_3$	− 2.96	− 3.95	− 1.91	− 4.94
Saleeite	$Mg(UO_2)_2(PO_4)_2$	–	–	− 12.05	− 12.92
Siderite	$FeCO_3$	− 4.32	− 4.84	− 2.95	− 4.44
Torbernite	$Cu(UO_2)_2(PO_4)_2$	–	–	− 13.78	− 11.35

organic matter through complexation and mineral formation (e.g., Rios-Arana et al. 2003; Mibus et al. 2007; Cumberland et al. 2016; Wang et al. 2017), which may slow down uranium transport to downstream and also to downgradient aquifers (Dangelmayr et al. 2017).

Generally, As has a $logK_d$ (Table 5) higher than the median of 2.5 (USEPA 2005), which is consistent with predominant As (V) species (Table 2) that promotes its adsorption in stream sediments. Indeed, As and Fe concentrations in DPL stream sediments remain approximately constant, while there is a slight decrease in the average As content in DPL surface waters (Appendix A, Table 4, Fig. 6). Most studies reported the decrease of trace elements with distance from the potential contamination source (e.g., Wang et al. 2017). However, this is not observed in the abandoned Barrôco D. Frango mining area. Arsenic, U and Th contents in stream sediments are an evidence of their role in the immobilization of these elements, reducing their concentration in DPL waters (Table 4, Fig. 6).

Moreover, the highest As and U contents in water are observed during winter (January 2017) and spring (March 2016), respectively, with higher Eh values, when oxidation and adsorption of these elements should have occurred (Appendix A). Although reductive dissolution of Fe (III) (hydr)oxides is recognized as a major remobilization mechanism for adsorbed As and U, sorption is highly dependent on various factors such as the pH, competition from other anions for sorption sites and solute concentrations (Hering and Dixit 2005; Yusan and Erenturk 2011; Marshall et al. 2014). Therefore, the Eh does not seem to be the unique parameter that influences the adsorption/desorption of As and U in the aquatic system of the abandoned Barrôco D. Frango mining area.

The mean $logK_d$ of Co, Cr, Cu and Pb is lower than the mean $logK_d$ of these elements from USEPA (2005), which is related to the predominant divalent forms (Table 2) and, consequently, to be released from sediments to the overlying water. Chromium occurs as trivalent form, the most toxic and mobile form, which is consistent with a $logK_d$ ranging from 2.63 to 3.06, and lower than the median value of 4.5 (USEPA 2005) (Table 5). The $logK_d$ of Zn suggests a tendency to be adsorbed by sediments, which is indicated by a gradual decrease in DPL water and stream sediments (Appendix A). The partition coefficients suggest that most elements (Th, Co, Cr, Cu and Pb) tend to be in solution, which contributes to their dispersion and subsequent water quality degradation. Moreover, the texture, mineralogy and chemical composition of stream sediments

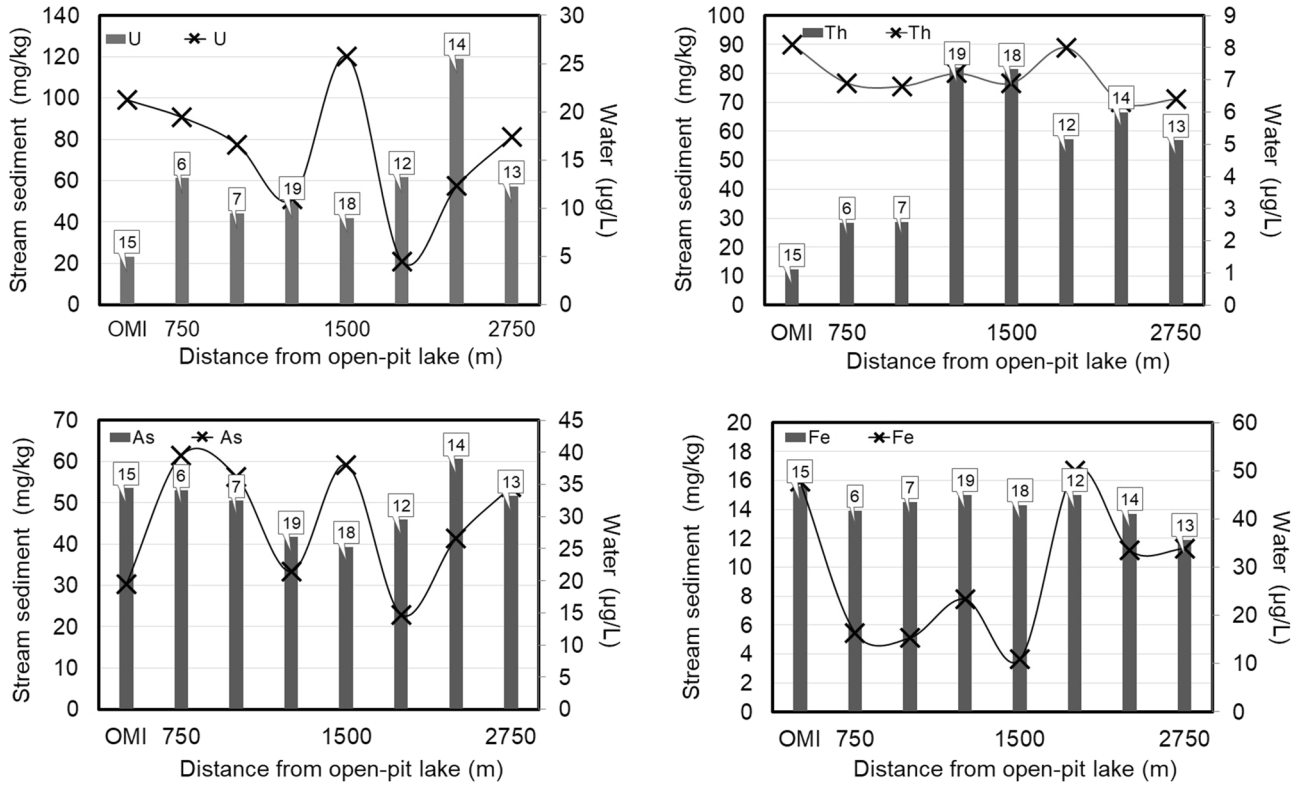

Fig. 6 Variation of the U, Th, As and Fe contents in waters and stream sediments from Barrôco D. Frango with the distance from the open-pit lake. Samples 15, 6, 7, 19, 18, 12, 14 and 13 correspond to water and stream sediment samples collected in the same location and in the same season (March 2016). OMI—outside the mining influence; X—surface waters; ■—stream sediments

are also very important in water quality management and the definition of remediation strategies.

Estimation of quality indicators and ecological risk assessment

Generally, DPL stream sediment samples have higher geoaccumulation (Igeo) values for metals; however, an identical or even a similar to slightly higher Igeo value for As than those of the OMI stream sediment sample (Tables 1 and 6). DPL stream sediment samples are moderately contaminated in As, moderately to heavily contaminated in Th, heavily to extremely contaminated in U and moderately to extremely contaminated in W (Table 6).

The potential ecological risk index (RI) evaluates the toxicity of potentially toxic elements for the biological community and is a relevant diagnostic tool for water pollution control purposes. The stream sediments from Barrôco D. Frango present a low contamination (C_f) for Co, Cr, Cu and Ni, low to moderate contamination in Al, Fe, Pb and Zn, low to considerable contamination in Mn, considerable to very high contamination in As and Th, and very high contamination in U and W (Tables 1 and 7). The C_d ranges from 24 to 209, which is higher than 20, therefore sediments show a very high degree of contamination (Tables 1 and 7). Arsenic, Th, U, and W are the trace elements that contribute to the highest C_d values.

Stream sediments show a low potential ecological risk factor (E_R^i) in Cr, Cu, Ni, Pb and Zn, but considerable to high E_R^i in As (Tables 1 and 8). The RI values range from 34 to 79; therefore, stream sediments have a moderate to considerable potential ecological risk index (Tables 1 and 8). Arsenic causes the most serious potential ecological risk in the DPL sediments from the old uranium Barrôco D. Frango mine area. Appropriate and ecological measures must be considered to reduce the As contents in the stream sediments. In other abandoned uranium mines, the potential ecological risk is also posed by U and As that have been reported as indicators of element fate and transport within aquatic systems (e.g., Kipp et al. 2009; Yi et al. 2020).

Stream sediment and water quality assessment

Some OMI and DPL water samples contain Cd (up to 30.1 µg/L) and Mn (up to 555 µg/L) contents higher than the recommended values for agricultural use (Appendix A). In the waters located in both areas, Cd, Cu, Fe, Mn and

Table 4 Textural characteristics, physical–chemical parameters, potentially toxic elements of stream sediments from the abandoned Barrôco D. Frango uranium mine area

Sample	Textural characteristics				Physical–chemical parameters					(mg/kg), except Al and Fe (g/kg)													
	% gravel	% sand	% silt	% clay	pH	EC (µS/cm)	T (°C)	OM (%)	CEC (cmol/Kg)	Al	Fe	As	Co	Cr	Cu	Mn	Ni	Pb	Sr	Th	U	W	Zn
Outside the mining influence																							
S15	19.4	75.6	4.57	0.42	5.54	41	22.4	2.8	3.6	16.3	15.6	53.5	2.9	3.7	3.9	277	3.1	27.0	9.8	12.3	23.2	*	47.3
Downstream of the open-pit lake and dump																							
S1	10.5	79.8	8.8	0.9	6.10	28	22.4	0.96	6.7	17.7	31.0	55.6	3.3	6.3	*	444	5.0	17.5	11.2	49.0	189	3.4	126
S2	n.d	n.d	n.d	n.d	5.15	54	22.4	n.d	n.d	10.4	8.1	25.4	*	*	2.3	84.3	2.1	16.7	7.3	27.2	51.2	*	45.8
S5	n.d	n.d	n.d	n.d	5.19	50	22.4	n.d	n.d	21.9	11.9	46.9	3.3	4.6	3.6	139	4.7	28.1	11.4	27.6	51.5	6.8	78.4
S6	34.6	59.8	5.0	0.5	7.23	20	22.3	0.47	1.7	18.3	13.9	53.0	4.1	5.2	8.6	629	4.1	30.2	16.4	28.4	61.2	3.4	73.5
S7	n.d	n.d	n.d	n.d	6.29	55	22.4	n.d	n.d	20.1	14.5	50.5	3.5	4.5	4.7	245	3.8	28.9	12.7	28.7	44.1	10.2	71.9
S9	n.d	n.d	n.d	n.d	6.48	99	22.3	n.d	n.d	19.3	15.3	50.6	4.6	5.0	6.8	559	2.4	25.6	19.0	32.1	53.3	*	67.5
S19	n.d	n.d	n.d	n.d	6.75	22	22.4	n.d	n.d	15.4	15.0	41.7	4.1	2.9	2.9	1411	2.3	18.7	11.7	81.9	49.4	42.1	51.3
S18	n.d	n.d	n.d	n.d	5.79	25	22.3	n.d	n.d	15.2	14.3	39.3	4.1	3.3	3.6	998	3.5	17.4	8.0	81.4	41.9	50.6	52.9
S12	11.7	85.8	2.3	0.3	6.65	29	22.5	0.72	2.4	17.2	15.0	45.9	4.5	3.0	3.6	341	4.1	23.5	12.0	57.3	61.5	6.7	53.0
S14	11.3	86.3	2.2	0.2	6.37	25	22.6	0.64	2.9	13.7	13.7	60.6	3.4	2.4	2.6	320	3.0	35.0	8.0	66.6	119	4.0	48.7
S13	9.0	90.8	0.17	0.02	6.57	12	22.5	0.22	1.3	11.0	11.9	51.6	4.5	*	2.1	893	2.9	10.6	7.8	56.9	57.1	81.5	62.3
ANZECC (mg/kg)										–	–	20	–	80	65	–	21	50	–	–	–	–	200

EC—electrical conductivity; OM—organic matter; CEC—cation exchange capacity; n.d.—not determined; *—below the detection limit. Detection limits in mg/Kg for Al 1.96, As 2.8, Cd 0.77, Co and Mn 2.2, Cr 2.3, Cu and U 2.0, Fe 1.29, Ni 1.92, Pb 2.1, Sb 1.14, Sr 1.76, Th 2.4, W 1.55 and Zn 0.70. Cd and Sb were not detected. Analyst: A.C.T. Santos. Target limits proposed by the Australian and New Zealand Environment and Conservation Council, ANZECC (2013)

Table 5 Partition coefficient (log K_d) ($L.kg^{-1}$) of potentially toxic elements in stream sediments and waters from Barrôco D. Frango

	As	Co	Cr	Cu	Pb	Th	U	Zn
downstream of the open-pit lake and dump								
SD6	3.13	3.03	3.06	3.35	3.55	3.61	3.50	4.49
SD7	3.14	2.98	2.97	3.24	–	3.63	3.42	4.35
SD9	3.31	3.05	3.04	3.24	3.53	3.71	3.64	4.60
SD12	3.49	3.01	2.74	–	3.77	3.86	4.14	4.56
SD13	3.17	2.95	–	2.56	3.20	3.95	3.52	4.50
SD14	3.36	2.78	2.63	–	3.53	4.02	3.99	–
SD18	3.01	2.96	2.76	3.19	3.34	4.07	3.21	4.56
SD19	3.29	2.98	2.73	2.97	-	4.06	3.66	4.54
Mean	3.24	2.97	2.85	3.09	3.49	3.86	3.63	4.51
Median*	2.5	3.3	4.5	4.2	5.1	–	–	3.7
Range*	1.6–4.3	2.9–3.6	–	0.7–6.2	2.0–7.0	–	–	1.5–6.2
Mean**	–	4.6	–	–	–	5.28	0.7	2.7
Range**	–	3.7–5.6	–	–	–	3.1–7.4	1.3–3.0	3.0–4.0

– not defined

*USEPA 2005

**IAEA 2010

U concentrations are also higher than the permitted values for human consumption (Portuguese Decrees 1998, 2007, 2017) and (WHO 2017). Some DPL water samples should not be used for human consumption due to Al and As contents (Appendix A). The water from open-pit lake is not recommended for irrigation due to high Mn contents, and should not be used for human consumption due to the high Cd and As concentrations. Some OMI and DPL water samples have U concentrations higher than 20 µg/L and 17 µg/L, respectively, and should not be used for human consumption (Appendix A; Health Canada 2017; NHMRC, NRMMC 2011).

Stream sediments contain lower Cr, Cu, Ni, Pb, and Zn contents than the Australian and New Zealand guideline values (ANZECC 2013) (Table 4). However, As contents exceed the trigger value of 20 mg/kg (ANZECC 2013) (Table 4).

Table 6 Geo-accumulation (Igeo) index for potentially toxic elements of stream sediments from the abandoned Barrôco D. Frango uranium mine area

Sample	Igeo values							Igeo-Classes						
	As	Mn	Pb	Th	U	W	Zn	As	Mn	Pb	Th	U	W	Zn
Outside the mining influence														
SD15	2.0	− 1.2	− 0.1	0.7	2.6	n.d	-1.2	2	0	0	1	3	n.d	0
Downstream of the open-pit lake and dump														
SD1	2.0	− 0.5	− 0.7	2.7	5.7	2.2	0.2	2	0	0	3	6	3	1
SD2	0.9	− 2.9	− 0.8	1.9	3.8	n.d	− 1.3	1	0	0	2	4	n.d	0
SD5	1.8	− 2.1	0.0	1.9	3.8	3.2	− 0.5	2	0	0	2	4	4	0
SD6	2.0	0.0	0.1	1.9	4.0	2.2	− 0.6	2	1	1	2	4	3	0
SD7	1.9	− 1.3	0.0	1.9	3.6	3.8	− 0.6	2	0	1	2	4	4	0
SD9	1.9	− 0.1	− 0.2	2.1	3.8	n.d	− 0.7	2	0	0	3	4	n.d	0
SD19	1.6	1.2	− 0.6	3.5	3.7	5.8	− 1.1	2	2	0	4	4	6	0
SD18	1.5	0.7	− 0.7	3.4	3.5	6.1	− 1.1	2	1	0	4	4	6	0
SD12	1.8	− 0.9	− 0.3	2.9	4.0	3.2	− 1.1	2	0	0	3	4	4	0
SD14	2.2	− 1.0	0.3	3.2	5.0	2.4	− 1.2	3	0	1	4	5	3	0
SD13	1.9	0.5	− 1.4	2.9	3.9	6.8	− 0.8	2	1	0	3	4	6	0

Igeo values for Al, Co, Cr, Cu, Fe, Ni and Sr concentrations are < 0. The Igeo class is 0 for them. n.d.—not determined for elements below the detection limit

Comparison with other old uranium mines in central Portugal and worldwide

In this section, a comparative study of stream sediments and waters from abandoned Barrôco D. Frango, Vale de Abrutiga, Mondego Sul and Mortórios uranium mine areas located in central Portugal (Fig. 1c) and others located worldwide is performed. All abandoned uranium mines from Portugal were exploited by open-pit, during the second half of century XIX. The rejected material was abandoned at the surface or discarded into the streams. All the four abandoned Portuguese uranium mines were located in the granitic rocks from the uraniferous geochemical province of central Portugal. Other abandoned uranium mines worldwide with different geological settings are presented (Table 9). This comparison shows the chemical fingerprints for the pollution in surface waters and stream sediments from abandoned U mines.

Table 7 Contamination factor (C_f) and degree of contamination (C_d) of potentially toxic elements in the stream sediments from abandoned Barrôco D. Frango uranium mine area

	Al	Fe	As	Co	Cr	Cu	Mn	Ni	Pb	Th	U	W	Zn	C_d
Outside the mining influence														
SD15	1.03	0.64	5.94	0.32	0.16	0.18	0.67	0.16	1.42	2.46	9.28	–	0.64	24
Downstream of the open-pit lake and dump														
SD1	1.11	1.27	6.18	0.37	0.27	–	1.08	0.26	0.92	9.80	75.60	6.80	1.70	106
SD2	0.65	0.33	2.82	–	–	0.10	0.21	0.11	0.88	5.44	20.48	–	0.62	32
SD5	1.38	0.49	5.21	0.37	0.20	0.16	0.34	0.25	1.48	5.52	20.60	13.60	1.06	51
SD6	1.15	0.57	5.89	0.46	0.23	0.39	1.53	0.22	1.59	5.68	24.48	6.80	0.99	51
SD7	1.26	0.59	5.61	0.39	0.20	0.21	0.60	0.20	1.52	5.74	17.64	20.40	0.97	56
SD9	1.21	0.62	5.62	0.51	0.22	0.31	1.36	0.13	1.35	6.42	21.32	–	0.91	41
SD19	0.97	0.61	4.63	0.46	0.13	0.13	3.43	0.12	0.98	16.38	19.76	84.20	0.69	133
SD18	0.96	0.58	4.37	0.46	0.14	0.16	2.43	0.18	0.92	16.28	16.76	101.20	0.71	146
SD12	1.08	0.61	5.10	0.50	0.13	0.16	0.83	0.22	1.24	11.46	24.60	13.40	0.72	61
SD14	0.86	0.56	6.73	0.38	0.10	0.12	0.78	0.16	1.84	13.32	47.60	8.00	0.66	82
SD13	0.69	0.49	5.73	0.50	–	0.10	2.17	0.15	0.56	11.38	22.84	163.00	0.84	209

Table 8 Potential ecological risk factor (E_R^i) of As, Cr, Cu, Ni, Pb and Zn in the stream sediments from Barrôco D. Frango

	As	Cr	Cu	Ni	Pb	Zn	$RI = \sum_{i=1}^{6} E_R^i$
Outside the mining influence							
SD15	59.44	0.32	0.89	0.82	7.11	0.64	69
Downstream of the open-pit lake and dump							
SD1	61.78	0.55	–	1.32	4.61	1.70	70
SD2	28.22	–	0.52	0.55	4.39	0.62	34
SD5	52.11	0.40	0.82	1.24	7.39	1.06	63
SD6	58.89	0.45	1.95	1.08	7.95	0.99	71
SD7	56.11	0.39	1.07	1.00	7.61	0.97	67
SD9	56.22	0.43	1.55	0.63	6.74	0.91	66
SD19	46.33	0.25	0.66	0.61	4.92	0.69	53
SD18	43.67	0.29	0.82	0.92	4.58	0.71	51
SD12	51.00	0.26	0.82	1.08	6.18	0.72	60
SD14	67.33	0.21	0.59	0.79	9.21	0.66	79
SD13	57.33	–	0.48	0.76	2.79	0.84	62
Minimum	28.22	0.21	0.48	0.55	2.79	0.62	34
Maximum	67.33	0.55	1.95	1.32	9.21	1.70	79
Mean	53.20	0.36	0.92	0.90	6.12	0.88	62
Reference (unpolluted)	10.00	2.00	5.00	5.00	5.00	1.00	28

RI potential ecological risk index

Table 9 Characteristics of abandoned uranium mine areas from Beiras area, central Portugal and worldwide and U concentrations in stream sediments and surface waters

Location	Main minerals exploited	Ore grade	Type of exploration	Host rock	Period of exploitation	Uranium produced	Tailings	Sediment sampling Date	Digestion method for sediments	Stream sediments U (mg/kg)	Water sampling Date	Surface waters U (µg/L)	References
Barrôco D. Frango, Guarda county, Portugal	Autunite and torbernite	up to 1.31 % U_3O_8	Open-pit	Breccia enriched in Fe, consisting of quartz and granite	1988–1989	ca. 20.8 tonnes of U_3O_8	40,020 m^3	2016	Aqua regia 1:3 HNO_3:HCL	41.9–189 (median 53.3)	2016–2017	4.5–37.3	This study
Vale de Abrutiga, Coimbra county, central Portugal	Saleeite and meta-saleeite	–	Open-pit	Quartz veins	1982–1989	ca. 90 tonnes of U_3O_8	1,400,000 tonnes	1999	Tri-acid digestion	27.8–301 (median 58)	1999		Pinto et al. 2004
Mondego Sul, Coimbra county, central Portugal	Autunite, torbernite, meta-urano-circite, meta-saleeite	–	Open-pit	Quartz veins	1987–1991	ca. 75 tonnes of U_3O_8	425,000 tonnes	2010–2011	Aqua regia (3:1 HCl–HNO_3)	67.1–266 (median 85)	2008–2009		Neiva et al. 2016
Mortórios, Guarda county, central Portugal	Torbernite and autunite	0.18% U_3O_8 (average)	Open-pit	Weathered basic rock dykes	1982–1988	ca. 27 tonnes of U_3O_8	135,732 m^3	2014	Aqua regia (3:1 HCl–HNO_3)	47.4–81.5 (median 53.5)	2014–2015		Neiva et al. 2019
Mailuu Suu, Southwestern part of Kyrgyzstan, in the Fergana Valley	Pitchblende and nivenite	0.03% to over 0.5% U	Underground mine	Bituminous limestone-type with structure controlled uranium mineralization in hydrocarbon-bearing carbonates	1946–1968	10 000 t U from 9.1 million t of ore	3,000,000 m^3		–	–		3.1–5.4	Corcho Alvarado et al. 2014; Dahlkamp 2009

Table 9 (continued)

Location	Main minerals exploited	Ore grade	Type of exploration	Host rock	Period of exploitation	Uranium produced	Tailings	Sediment sampling Date	Digestion method for sediments	Stream sediments U (mg/kg)	Water sampling Date	Surface waters U (µg/L)	References
La Commanderie uranium mine, western France near the village of "Le Temple"	Pitchblende	–	Underground mining operations (1955–1990) and open-pit mine (1964–1977)	Granitic bedrock	1955–1990	3.644 thousand tons (kt) of U_3O_8	4.96 Mt of tailings		–	–		9.0–436	Martin et al. 2019
Olšíe Drahonín (Czech Republic)	Uraninite and coffinite	0.25 % U	Underground mine	Migmatized biotite gneiss and amphibolite	1957–2003	16,120 t U (Rožna); 2,735 t U (Olšíe) of U_3O_8	–	2010	A mixture of ultra pure HCl (3 mL) and ultra pure HNO_3(1 mL)	44.3–232	2003–2010	4.30–329	Hudcová et al. 2013
Bertholène mine, Palanges, Massif Central, France	Coffinite and pitchblende	–	Underground (1981–1992) and open- pit (1983–1995)	Palanges Precambrian orthogneiss	1981–1995	744 tons of uranium	470,000 tons	–	$HClO_4$ + HNO_3 + HF + HCl	4.4–273	–	–	Cuvier et al. 2016; Schmitt and Thiry 1987; Lévêque et al. 1988
Northern Guangdong Province, China	Uraninite	5–13 µg/g	–	Guidong Granite Massif, diabase dikes and silicified fracture zones	Recent	–	0.1 million tons	2016–2017	0.5 mol/L HCl	22.85–2700	–	–	Wang et al. 2017
Crucea ore deposit, in the East Carpathians, Romania	Pitchblende	–	Underground mine	Brecciated retrometamorphic micaschists, containing carbonates and clay minerals	1962–2004	1,200,000 tones of pitchblende ore	30 solid radioactive mining wastes	–	Lithium tetraborate 20%, lithium metaborate 80 %	17.20–5024	–	–	Petrescu et al. 2010

Table 9 (continued)

Location	Main minerals exploited	Ore grade	Type of exploration	Host rock	Period of exploitation	Uranium produced	Tailings	Sediment sampling Date	Digestion method for sediments	Stream sediments U (mg/kg)	Water sampling Date	Surface waters U (µg/L)	References
Edgemont U district, southern Black Hills of South Dakota, USA	Carnotite, corvusite, tyuyamunite, rauvite, autunite	0.2 % U_3O_8 (average)	Open-pit	Sandstone of the Lakota and Fall River Formations of early Cretaceous age	1951–1964	1 million tons of U_3O_8	–	–	X-rayfluorescence spectrometry (XRF)	17.40–52.40	–	0.08–44	Bell and Bales 1954; Williamson and Carter 2001; Sharma et al. 2016
Juniper Mine, Stanislaus River watershed of the Stanislaus National Forest in northern California	Coffinite, uraninite	up to 0.5% U_3O_8	Open- pit	Miocene volcanic Relief Peaks Formation, with heterogeneous andesite lahar and conglomerate beds.	1956–1966	45,500 pounds of U_3O_8	–	–	1:3 solution of concentrated HF:3MHNO$_3$	0.9681–22.1	2010	0.02223–52.37	Rapp and Short 1981; Kayzar et al. 2014
Ranger mine, Northern Australia	Uraninite with accessory coffinite and brannerite	1% U_30_8 (average)	Open- pit	Quartz schist, mica schist, paraamphibolite, calcsilicate and carbonate	1981–2012	5000 tonnes of U_3O_8	–	2007	10% HCl, concentrated HNO_3/$HClO_4$ mixture	0.02–18	2005–2008	0.01–0.13	Hein 2002; Bollhöfer 2012; Australian Government 2013

Stream sediments

DPL stream sediment samples from Barrôco D. Frango mine area have lower minimum, maximum and median U, Pb, Fe, Co, Cr, Cu and Zn contents and a higher median Th content than those of stream sediments from Vale de Abrutiga (Tables 9 and 10). Abandoned Barrôco D. Frango mine produced 69 fewer tons of U_3O_8 than the Vale de Abrutiga mine (Tables 9 and 10), which caused less impact on the environment.

DPL stream sediments from abandoned Barrôco D. Frango mine area have a lower median metal and the metalloid As contents than those from Mondego Sul (Tables 4 and 10), because it produced 56 fewer tons of U_3O_8 (Tables 9 and 10).

The stream sediments from Barrôco D. Frango also contain higher median Th, Pb and Zn contents and similar median U contents than those of stream sediments from Mortórios (Tables 9 and 10). The former produced 6 fewer tons of U_3O_8 than the latter (Table 9). Although the autunite and torbernite occur in both Barrôco D. Frango and Mortórios uranium mines. These mines are in weathered basic rock dykes. At Mortórios is associated with older quartz veins containing sulphides. At Barrôco D. Frango, the ore minerals occur in a breccia containing quartz, granite, Fe oxy-hydroxides and clays. The weathering of granite also contributes to the U and Th contents, because these metals occur in the accessory minerals' zircon, monazite, xenotime and apatite. However, the main impact must have been caused by the amount of autunite and torbernite, which certainly were higher in the breccia (Barrôco D. Frango) than in the weathered basic rocks, as the exploitation was carried on for one year in the breccia and seven years in the basic rock dykes.

A comparison of uranium contents in stream sediments from various abandoned uranium mines worldwide provides the relative impacts due to the uranium exploitation, concerning the geological settings, U production and main minerals exploited.

Stream sediments from Barrôco D. Frango (Portugal) present higher U contents than the stream sediments from Edgemont U district (USA), Juniper mine, (California) and Ranger mine, (Australia) (Table 9). Stream sediments from Olšíe Drahonín mine (Czech Republic) transport U contents (up to 232 mg/kg) similar to those of stream sediments from Barrôco D. Frango area (up to 189 mg/kg). However, surface waters from Olšíe Drahonín mine reach much higher uranium contents (329 µg/L) (Table 9) than those from Barrôco D. Frango. This may be evidence of the low U retention capacity of stream sediments. Since Olšíe Drahonín mine produced more uranium than Barrôco D. Frango mine, surface waters from Olšíe Drahonín area are the most affected by U pollution.

However, uranium contents in stream sediments from Northern Guangdong Province (China), and Crucea mine (Romania) are 14 and 25 times higher than U contents in stream sediments from Barrôco D. Frango (Table 9). Both mines exploited more U than Barrôco D. Frango mine. However, the Bertholène mine (France), with a significantly higher U production than that of Barrôco D. Frango and, consequently larger volumes of mine wastes, have slightly higher U concentration in their stream sediments than those of the study area (Table 9). This is consistent with the effluent water treatment that were neutralized with lime, sodium hydroxide and flocculating agents, before being released into the Balaures stream (Cuvier et al. 2016).

Water samples

The cluster heat maps allowed the construction of crossed clusters for the geochemical composition of waters from the Portuguese four mines considered, namely for the open-pit water, groundwater and surface water (Fig. 7a–c). Considering the open-pit water, it is possible to define two significant clusters. The first aggregating pH, Eh, Mg, Cd, Cr, Ni, As and Th and the second aggregating EC, SO_4^{2-}, Cu, Fe, Mn, Pb, Zn and U (Fig. 7a). The corresponding heat map reveals that Mondego Sul and Barrôco D. Frango mines are the most similar in Fe, Cu, Mn, Zn, U, Pb and SO_4^{2-} contents. This is due to the similar ore minerals exploited in both mines, but essentially due to the contamination produced in waters, and similar pH values in two open-pit lakes. The pH values of the water from these two open-pit lakes define the group of metals in solution, with the tendency for the divalent species of metals to belong to the same group.

The Vale da Abrutiga mine is a singular case for surface and groundwaters, which can be explained by the high U_3O_8 production compared with the other three uranium mines (Table 9). Moreover, the main ore minerals exploited, saleeite and meta-saleeite, are different from those of the other three mines. Vale de Abrutiga mine produced waters from open-pit lake with the highest EC, 2962 µS/cm, about ten times more than EC of open-pit water from the other three mines. Thorium and U contamination in the water is also the most significant compared with the other three old Portuguese uranium mines.

The groundwater's cluster heat maps reveal three main clusters: the first one aggregating pH, Eh, Cd, Cr, Ni, As, Th; the second one aggregating EC, Cu, Fe, Mn, Pb, Zn and U; and the third one aggregating $SO_4^{2-}$and Mg (Fig. 7b). Mondego Sul and Barrôco D. Frango mines are again the most similar, namely for Mn, Fe, U, Zn, Cu and Pb contents in water. The compositional trend for Barrôco D. Frango and Mondego Sul groundwater is similar to surface water, with

Table 10 Basic statistical parameters of potentially toxic element contents (ppm) in DPL stream sediments from the abandoned uranium mine areas of Vale de Abrutiga, Mondego Sul, Mortórios and Barrôco D. Frango

	Vale de Abrutiga			Mondego Sul			Mortórios			Barrôco D. Frango		
	Min.	Max.	Median	Min.	Max.	Median	Min.	Max.	Median	Min.	Max.	Median
Th	3.3	10.8	9.6	115	281	180	13.0	68.2	19.5	27.2	81.9	49.0
As	n.d	n.d	n.d	49.0	211	118	35.4	83.2	59.4	25.4	60.6	50.5
Pb	25.0	44.0	38.0	25.1	159	55.7	9.3	14.3	11.6	10.6	35.0	23.5
Fe (%)	2.7	23.9	3.8	1.20	3.8	3.0	0.80	1.53	1.16	0.81	3.1	1.43
Co	11.0	74.0	16.0	8.7	47.4	12.6	*	5.1	3.1	*	4.6	4.1
Cr	70.0	107	99.0	14.2	66.1	37.2	4.6	15.7	12.9	*	6.3	4.5
Cu	18.1	66.5	41.7	18.3	47.4	29.7	*	8.9	7.7	*	8.6	3.6
Zn	130	803	158	78.2	346	126	44.8	54.6	49.9	45.8	126	62.3

Min. minimum, *Max.* maximum

*Below the detection limit

near-neutral pH values (6.2 and 6.0, respectively) and very similar mean metal concentrations (Appendix A).

The surface water's cluster heat maps identify three main clusters: the first one aggregating pH, Eh, Mg, Cd, Cr and Ni; the second one aggregating EC, SO_4^{2-}, Cu, Fe, Mn, Pb, Zn and U; and the third one aggregating As and Th (Fig. 7c). The Mondego Sul and Barrôco D. Frango mines are again the most similar, namely for the content in Mn, Fe, U, Zn, Cu, Pb and SO_4^{2-}. Excluding SO_4^{2-} contents, surface water and groundwater from Mondego Sul and Barrôco D. Frango are characterized by high Mn, Fe, U, Zn, Cu, Pb contents. The divalent form of these metals tends to occur in waters and high levels of uncharged uranium carbonate can result.

Concerning surface water U contents, those from Barrôco D. Frango present lower U concentrations than most surface waters from U mine areas worldwide (Table 9). Only the mines of Mailuu Suu (Kyrgyzstan) and Range Mine (Australia), with lower U contents in surface waters than those from Barrôco D. Frango, are an exception. In these two mining areas, the geological setting may have influenced the uranium contents dispersed in the environment, with geological formations containing carbonates that may increase the pH values of the water drainage (Table 9). However, in all mining areas, a common feature seems to be evident, namely that mines with higher uranium exploitation tend to have greater contamination impacts, unless the geology is favorable to the retention of contaminants or even a remediation treatment that has been adopted to lower the drainage pH values.

Conclusions

In this study, the pollution degree and water–stream sediment interaction that occurred in abandoned uranium mines in central Portugal were investigated. The abandoned uranium mines are located in a very important uraniferous geochemical region in Portugal, where other uranium mines were also abandoned. In these old mines, open-pit and mine dumps were left in the area, without any remediation procedures.

The results obtained in this study shows that U, Th and As contents in the open-pit water are similar to those of downstream water, which shows its influence in downstream aquatic systems. In downstream sediment, the partition coefficients determined in Bârroco D. Frango suggest the adsorption of U and As by Fe-oxy-hydroxides precipitated from waters. In most abandoned mines, stream sediment is moderately to heavily contaminated in U, Th and As. Generally, in old U mines, potentially toxic elements tend to decrease their contents downstream mine influence. However, in Barrôco D. Frango area, U content in the stream sediments tends to increase. In this abandoned mine area, the RI ranges from 34 to 79; therefore, stream sediments have moderate to considerable potential ecological risk, mainly caused by arsenic, which exceeds up to 3 orders of magnitude the trigger value (20 mg/kg) reported in the guidelines of ANZECC (2013).

Despite the small U exploitation of some abandoned U mines in Portugal and their low U contents in water and stream sediments compared to other abandoned U mines worldwide, U, Th and As contamination of stream sediments and potential ecological risk are of concern. It places the sediments as central to the management of water quality and ecological risk. Additionally, climate changes may also pose risks to water management due to the potential water–sediment interaction modifications. Therefore, further studies should be carried out focusing on water–stream sediment interaction, understanding factors and processes that regulate water quality, especially under a climate change scenario.

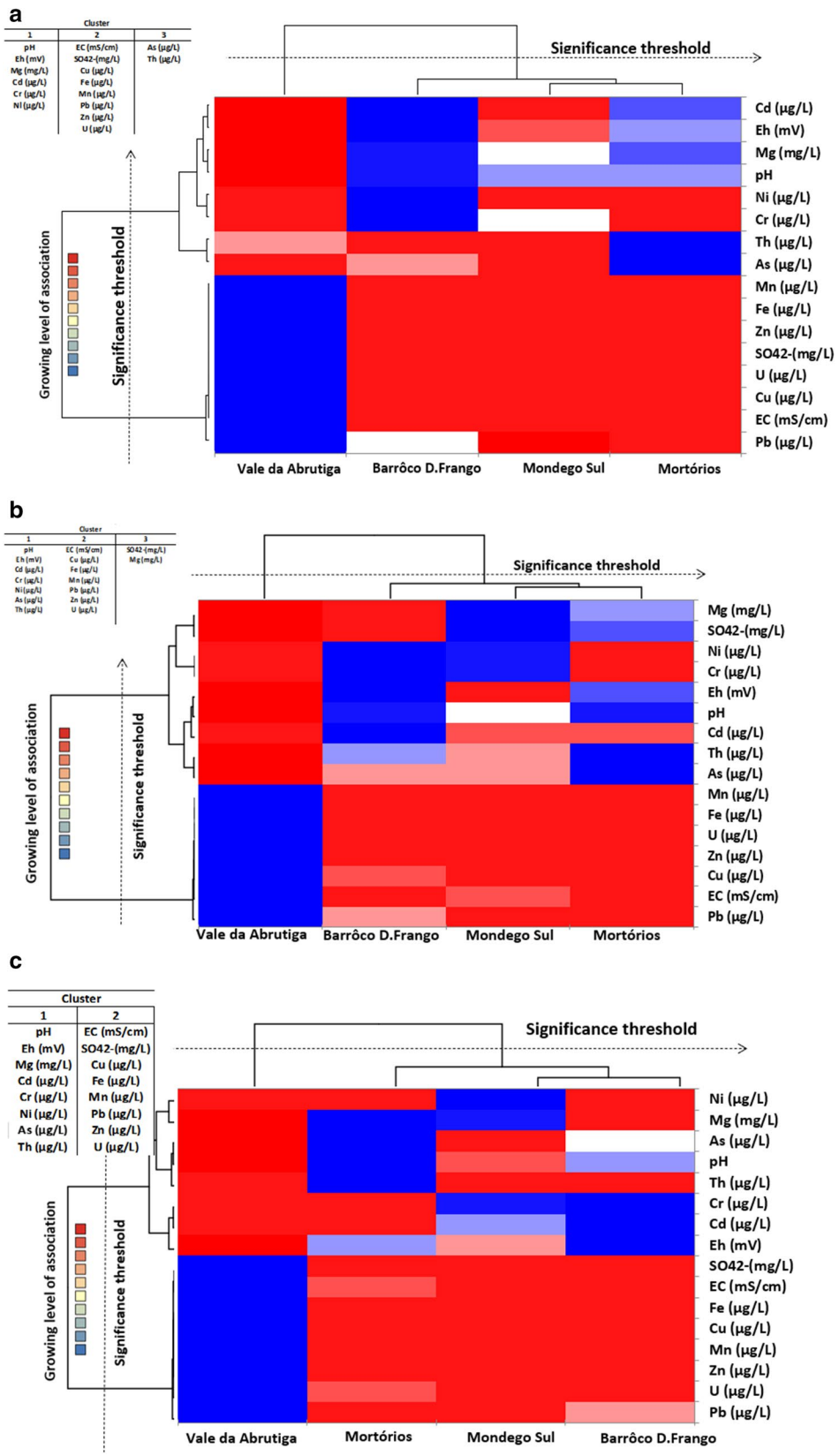

Fig. 7 Cluster heat maps: **a** Open-pit water; **b** Groundwaters; **c** Surface waters

Supplementary Information The online version contains supplementary material available at https://doi.org/10.1007/s12665-022-10275-2.

Acknowledgements This work was funded by the Fundação para a Ciência e Tecnologia (FCT), through (i) national funds, by the projects UID/GEO/04035/2016 — GeoBioTec- GeoBioSciences, GeoTechnologies and GeoEngineering, UIDB/04683/2020, UIDP/04683/2020 — ICT and UIDB/MAR/04292/2020 — MARE (Marine and Environmental Sciences Centre); (ii) a Sabbatical grant (ref. SFRH/BSAB/150395/2019) hold by Pedro P. Cunha (Programa Operacional Capital Humano). Ana Barbara Costa helped in the Sedimentology Laboratory, from the University of Coimbra and Carlos Maia produced the XRD of stream sediment samples. We are grateful to Dr. James Temple for reviewing the manuscript. We would also like this work to be a tribute to Professor Ana Neiva, the previous leader of our team, who passed away in 2019. The authors are grateful to anonymous referees for their constructive comments and suggestions, which greatly improved the manuscript.

Declarations

Conflict of interest The authors declare that they have no known competing financial interests or personal relationships that could have appeared to influence the work reported in this paper.

References

Addo-Bediako A, Nukeri S, Kekana M (2021) Heavy metal and metalloid contamination in the sediments of the Spekboom River. South Africa Appl Water Sci 11:133. https://doi.org/10.1007/s13201-021-01464-8

Antunes IMHR, Neiva AMR, Albuquerque MTD, Carvalho PCS, Santos ACT, Cunha PP (2018) Potential toxic elements in stream sediments, soils and waters in an abandoned radium mine (central Portugal). Environ Geochem Health 40:521–542. https://doi.org/10.1007/s10653-017-9945-2

Antunes IMHR, Teixeira RJS, Valente TMF, Santos ACT (2019) Geoaccumulation indexes of trace elements in sediments from uranium environments (Central Portugal). 2nd Conference of the Arabian Journal of Geosciences (CAJG), Springer Nature

Antunes IMHR, Santos ACT, Valente TMF, Albuquerque MTD (2020) Spatial mobility of U and Th in a U-enriched area (Central Portugal). Appl Sci 10(21):7866. https://doi.org/10.3390/app10217866

Antunes IMHR, Teixeira RJS, Albuquerque MTD, Valente TMF, Carvalho PCS, Santos ACT (2021) Water-rock interaction and potential contamination risk in a U-enriched area. Geosciences 2021:11

Astatkie H, Ambelu A, Mengistie E (2021) Contamination of stream sediment with heavy metals in the Awetu watershed of Southwestern Ethiopia. Front Earth Sci 9:609. https://doi.org/10.3389/feart.2021.658737

Australian and New Zealand Environment and Conservation Council (ANZECC) (2013) ANZECC interim sediment quality guidelines. Report for the Environmental Research Institute of the Supervising Scientist, Sydney

Australian Government (2013) Interim report: investigation into the environmental impacts of the leach tank failure at Ranger uranium mine. Department of the Environment. Supervising scientist report: 221

Bachmaf S, Merkel BJ (2011) Sorption of uranium (VI) at the clay mineral-water interface. Environ Earth Sci 63:925–934

Bargar JR, Reitmeyer R, Lenhart JJ, Davis JA (2000) Characterization of U(VI)-carbonato ternary complexes on hematite: EXAFS and electrophoretic mobility measurements. Geochim Cosmochim Acta 64:2737–2749

Barnett MO, Jardine PM, Brooks SC, Selim HM (2000) Adsorption and transport of uranium (VI) in surface media. Soil Sci Am J 64:908–917

Bell H, Bales WE (1954) Uranium deposits in Fall River Country, south Dakota. Trace Elements Investigations Report 297. United States Department of the Interior. Geological Survey

Bollhöfer A (2012) Stable lead isotope ratios and metals in freshwater mussels from a uranium mining environment in Australia's wet-dry tropics. Appl Geochem 27:171–185. https://doi.org/10.1016/j.apgeochem.2011.10.002

Bowell RJ (2002) The hydrogeochemical dynamics of mine pit lakes. In YOUNGER, EL. & ROBINS, N.S. (eds) 2002. Mine Water Hydrogeology and Geochemistry. Geological Society, London, Special Publications, 198, 159–185. The Geological Society of London 2002.

British standard (BS) 7755 (1995a) Soil quality, part 3. Chemical methods, section 3.2. Determination of pH. ISO 10390, 1995a

British standard (BS) 7755 (1995b) Soil quality, part 3. Chemical methods, section 3.4. Determination of specific electrical conductivity. ISO 11265, 1994

Brown RM, Mcclelland NI, Deininger RA, Tozer RG (1970) A water quality index: do we dare? Water Sewage Works 117(10):339–343

Calmuc VA, Calmuc M, Arseni M, Topa CM, Timofti M, Burada A, Iticescu C, Georgescu LP (2021) Assessment of heavy metal pollution levels in sediments and of ecological risk by quality indices, applying a case study: the lower Danube River. Romania Water 13:1801. https://doi.org/10.3390/w13131801

Health Canada (2017) Guidelines for Canadian drinking water quality-summary table. Water and air quality bureau, healthy environments and consumer safety branch, Health Canada, Ottawa, Ontario

Carvalho FP (2014) The National radioactivity monitoring program for the regions of uranium mines and uranium legacy sites in Portugal. Procedia Earth Planetary Sci 8:33–37

Carvalho FP, Malta M, Oliveira JM (2010) III. Programa específico para as regiões das minas de urânio. Relatório UPSR-A, nº 3710. Instituto Tecnológico e Nuclear, Unidade de Proteção e Segurança Radiológica: 101–146

Cerdas F, Kaluza A, Erkisi-Arici S, Böhmea S, Herrmann C (2017) Improved visualization in LCA through the application of cluster heat maps. Procedia CIRP 61:732–737

Cheng T, Barnett MO, Rodin EE, Zhuang Y (2007) Reactive transport of uranium (VI) and phosphate in a goethite-coated sand column: an experimental study. Chem 68:1218–1223

Chernov VA (1947) The nature of soil acidity. Soil Science Society of America, Madison, p 169p

Corcho Alvarado JA, Balsiger B, Rollin S, Jakob A, Burger M (2014) Radioactive and chemical contamination of the water resources in the former uranium mining and milling sites of Mailuu Suu (Kyrgyzstan). J Environ Radioact 138:1–10

Costa MR, Pereira AJSC, Neves LJPF, Fererira A (2017) Potential human health impact of groundwater in non-exploited uranium ores: the case of Horta da Vilariça (NE Portugal). J Geochem Expl 183(Part B):191–196. https://doi.org/10.1016/j.gexplo.2017.03.010

Cowart JB, Burnett WC (1994) The distribution of uranium and thorium decay-series radionuclides in the environmental—a review. J Env Qual 23:651–662

Cumberland SA, Douglas G, Grice K, Moreau JW (2016) Uranium mobility in organic matter-rich sediments: a review of geological and geochemical processes. Earth-Sci Rev 159:160–185

Cuvier A, Pourcelot L, Probst A, Prunier J, Le Roux G (2016) Trace elements and Pb isotopes in soils and sediments impacted by uranium mining. Sci Total Environ 566–567:238–249

Dahlkamp FJ (2009) Kyrgyzstan. In: Dahlkamp FJ (ed) Uranium deposits of the world. Springer, Berlin

Dangelmayr MA, Reimus PW, Wasserman NL, Punsal JJ, Johnson RH, Clay JT, Stone JJ (2017) Laboratory column experiments and transport modelling to evaluate retardation of uranium in an aquifer downgradient of a uranium in situ recovery site. Appl Geochem 80:1–13

Portuguese Decree (1998) Decree 236/1998. Portuguese legislation on water quality. Diário da República I-A: 3676–3722

Portuguese Decree (2007) Portuguese legislation on water quality. Diário da República I-A: 5747–5765

Portuguese Decree (2017) Portuguese Legislation on Water Quality. Diário da República I-A, Lisbon, nº 235: 6555–6576

Devaraj N, Banajarani P, Chidambaram S, Prasanna MV, Dhiraj Kr S, Ramanathan AL, Sahoo SK (2021) Spatio-temporal variations of Uranium in groundwater: implication to the environment and human health. Sci Total Environ 775:145787. https://doi.org/10.1016/j.scitotenv.2021.145787

Dong WM, Brooks SC (2006) Determination of the formation constants of ternary complexes of uranyl and carbonate with alkaline earth metals (Mg2+, Ca2+, Sr2+, and Ba2+) using an-ion exchange method. Environ Sci Technol 40:4689–4695. https://doi.org/10.1021/es0606327

Eary LE (1999) Geochemical and equilibrium trends in mine pit lakes. Appl Geochem 14:963–987

EDM (2017) Remediação ambiental da área mineira de Barrôco D. Frango. Estudos, projetos e obras. http://edm.pt/area-ambiental/estudos-projetoseobras

European Commission (2011) Uranium sites. Environmental radioactivity and discharge monitoring and part of national monitoring system for environmental radioactivity. Portugal. Technical report. Reference PT-11/01

Feng C, Guo X, Yin S, Tian C, Li Y, Shen Z (2017) Heavy metal partitioning of suspended particulate matter-water and sediment-water in the Yangtze Estuary. Chemosphere 185:717–725. https://doi.org/10.1016/j.chemosphere.2017.07.075

Ferreira AMPJ (2000) Dados geoquímicos de base de sedimentos fluviais de amostragem de baixa densidade de Portugal Continental: Estudo de factores de variação regional. Unpublished PhD thesis, Univ. Aveiro, Portugal

Gavrilescu M, Pavel LV, Cretescu I (2009) Characterization and remediation of soils polluted with uranium. J Hazard Mater 163:475–510

Geipel G, Amayri S, Bernhard G (2008) Mixed complexes of alkaline earth uranyl carbonates: a laser-induced time-resolved fluorescence spectroscopic study. Spectrochim Acta A 71:53–58. https://doi.org/10.1016/j.saa.2007.11.007

Gómez P, Garralón A, Buil B, Turrero MJ, Sánchez L, De la Cruz B (2006) Modeling of geochemical processes related to uranium mobilization in the groundwater of a uranium mine. Sci Total Environ 366:295–309

Håkanson L (1980) An ecological risk index aquatic pollution control. A sedimentological approach. Water Res 14:975–1001

Hein KAA (2002) Geology of the Ranger Uranium Mine, Northern Territory Australia: structural constraints on the timing of uranium emplacement. Ore Geol Rev 20:83–108

Hering JG, Dixit S (2005) Contrasting sorption behavior of arsenic (III) and arsenic (V) in suspensions of iron and aluminium oxyhydroxides. P.A. O'Day, D. Vlassopoulos, X. Meng, L.G. Benning (Eds.), Advances in Arsenic Research, Chapter 2: 8–24

Hsi C-KD, Langmuir D (1985) Adsorption of uranyl onto ferric oxyhydroxides: applications of the surface complexation site-binding model. Geochim Cosmochim Acta 49:1931–1941

Hsu LC, Huang CY, Chuang YH et al (2016) Accumulation of heavy metals and trace elements in fluvial sediments received effluents from traditional and semiconductor industries. Sci Rep 6:34250. https://doi.org/10.1038/srep34250

Hudcová H, Badurová J, Rozkosný M, Sova J, Funková R, Svobodová J (2013) Quality and mutagenicity of water and sediment of the streams impacted by the former uranium mine area Olší-Drahonín (Czech Republic). J Environ Radioact 116:159–165

IAEA (2010) Handbook of parameter values for the prediction of radionuclide transfer in terrestrial and freshwater environments. International Atomic Energy Agency. Technical report series no. 472, Vienna, Austria

Jung HB, Yun ST, Mayer B et al (2005) Transport and sediment–water partitioning of trace metals in acid mine drainage: an example from the abandoned Kwangyang Au–Ag mine area, South Korea. Environ Geol 48:437–449. https://doi.org/10.1007/s00254-005-1257-7

Junta de Energia Nuclear (1957) Jazigo de Barrôco D. Frango. Relatório de execução do plano de sanjas, nº 72. Serviço de Prospecção da J.E.N., 2ª Brigada de Prospecção

Kayzar TM, Villa AC, Lobaugh ML, Gaffney AM, Williams RW (2014) Investigating uranium distribution in surface sediments and waters: a case study of contamination from the Juniper Uranium Mine, Stanislaus National Forest. CA J Environ Radioact 136:85–97

Kipp GG, Stone JJ, Stetler LD (2009) Arsenic and uranium transport in sediments near abandoned uranium mines in Harding County, South Dakota. Appl Geochem 24(12):2246–2255. https://doi.org/10.1016/j.apgeochem.2009.09.017

Kubiak J, Machula S (2014) Concentration of uranium in waters of the biggest lakes of the Tywa river drainage basin. J Ecol Eng 15(3):56–63. https://doi.org/10.12911/22998993.1109124

Langmuir D (1978) Uranium solution-mineral equilibria at low temperatures with applications to sedimentary ore deposits. Geoch Cosmoch Acta 42(6):547–569

Langmuir D (1997) Aqueous environmental geochemistry. Prentice Hall

Lévêque MH, Lancelot JR, George E (1988) The bertholène uranium deposit mineralogical characteristics and U-Pb dating of the primary U mineralization and its subsequent remobilization: consequences upon the evolution of the U deposits of the Massif Central. France Chem Geol 69:147–163

Li D, Kaplan DI (2012) Sorption coefficients and molecular mechanisms of Pu, U, Np, Am and Tc to Fe (hydr)oxides: a review. J Hazard Mater 243:1–18

Markich SJ (2002) Uranium speciation and bioavailability in aquatic systems: an overview. Sci World J 2:707–729

Marshall TA, Morris K, Law GTW, Livens FR, Mosselmans JF, Bots P, Shaw S (2014) Incorporation of uranium into hematite during crystallization from ferrihydrite Environ. Sci Technol 48(7):3724–3731

Martin A, Landesman C, Lépinay A, Roux C, Champion J, Chardon P, Montavon G (2019) Flow period influence on uranium and trace elements release in water from the waste rock pile of the former La Commanderie uranium mine (France). Journal of Environmental Radioactivity. 208–209. 106010.

Mibus J, Saches S, Pfingsten W, Nebelung C, Bernhard G (2007) Migration of uranium (IV)/(VI) in the presence of humic acids in quartz sand: a laboratory column study. J Contam Hydrol 89:199–217

Miranda LS, Ayoko GA, Egodawatta P, Hu WP, Ghidan O, Goonetilleke A (2021) Physico-chemical properties of sediments governing the bioavailability of heavy metals in urban waterways. Sci Total Environ 763:142984. https://doi.org/10.1016/j.scitotenv.2020.142984

Missana T, Garcia-Gutiérrez M, Alonso U (2004) Kinetics and irreversibility of cesium and uranium sorption onto bentonite colloids in a deeps granite environment. Appl Clay Sci 26:137–150

Mochizuki A, Hosoda K, Sugiyama M (2016) Characteristic seasonal variation in dissolved uranium concentration induced by the change of lake water pH in Lake Biwa, Japan. Limnology 17:127–142. https://doi.org/10.1007/s10201-015-0469-0

Mortvedt JJ (1994) Plant and soil relationships of uranium and thorium decay series radionuclides— a review. Environ Qual 23:643–650

Moyes LN, Parkman RH, Charnock DJ, Livens FT, Hughes CR, Braithwaite A (2000) Uranium uptake from aqueous solution by interaction with goethite, lepidocrocite, muscovite and mackinawite: An x-ray absorption spectroscopy study. Environ Sci Technol 34:1062–1068

Mühr-Ebert EL, Wagner F, Walther C (2019) Speciation of uranium: Compilation of a thermodynamic database and its experimental evaluation using different analytical techniques. Appl Geochem 100:213–222. https://doi.org/10.1016/j.apgeochem.2018.10.006

Müller G (1981) Die Schwermetallbelstung der sedimente des Neckars und seiner Nebenflusse: eine Bestandsaufnahme. Chem Ztg 105:156–164

Müller SN (1979) In: Den sediment des Rheins-Veranderungen seilt (1971). Unschau, 79, 778–783.

Neiva AMR, Carvalho PCS, Antunes IMHR, Silva MMVG, Santos ACT, Cabral Pinto MMS, Cunha PP (2014) Contaminated water, stream sediments and soils close to the abandoned Pinhal do Souto uranium mine, Central Portugal. J Geochem Explor 136:102–117

Neiva AMR, Carvalho PCS, Antunes IMHR, Santos ACT, Cabral-Pinto MMS (2015) Spatial and temporal variability of Surface water and groundwater before and after remediation of a Portuguese uranium mine area. Geochemistry 76:345–356. https://doi.org/10.1016/j.chemer.2016.08.003

Neiva AMR, Antunes IMHR, Carvalho PCS, Santos ACT (2016) Uranium and arsenic contamination in the former Mondego Sul uranium mine area, Central Portugal. J Geochem Explor 162:1–15

Neiva AMR, Carvalho PCS, Antunes IMHR, Albuquerque MTD, Santos ACT, Cunha PP, Henriques SBA (2019) Assessment of metal and metalloid contamination in the waters and stream sediments around the abandoned uranium mine area from Mortórios, central Portugal. J Geochem Explor 202:35–48. https://doi.org/10.1016/j.gexplo.2019.03.020

NHMRC, NRMMC (2011) Australian drinking water guidelines, paper 6 National water quality management strategy. National Health and Medical Research Council, National Resource Management Ministerial Council, Commonwealth of Australia, Canberra

Nordstrom DK, Wilde FD (2005) Reduction oxidation potential (electrode method). In Wilde, F.D. (ed.). Field measurements: U.S. Geological Survey Techniques of Water. Resources Investigations, book, chap. A6, version 1.2 (9/2005). https://water.usgs.gov/owq/FieldManual/Chapter6/6.5_V_1.2.pdf.

Nye P, Craig D, Coleman NT, Ragland JL (1961) Ion exchange equilibria involving aluminium. Soil Sci Am J 25:14–17

Panagiotaras D, Nikolopoulos D (2015) Arsenic occurrence and fate in the environment; a geochemical perspective. J Earth Sci Clim Change 6:269. https://doi.org/10.4172/2157-7617.1000269

Parkhurst DL, Appelo CAJ (1999) User's Guide to PHREEQC (Version 2)—A Computer Program for Speciation, Batch-Reaction, One-Dimensional Transport, and Inverse Geochemical Calculations. U.S. Geological Survey, Water Resources Investigations Report 99–4259, Washington DC

Parra A, Filipe A, Falé P (2002) Sistema de Informacão de Ocorrência de Recursos Minerais Portugueses-SIORMINP. Instituto Geológico Mineiro, Lisboa.

Pereira R, Barbosa S, Carvalho FP (2014) Uranium Mining in Portugal: a Review of the Environmental Legacies of the Largest Mines and Environmental and Human Health Impacts. 9Th International Symposium on Environmental Geochemistry 36: 285–301

Petrescu L, Bilal E, Iatan LE (2010) The impact of a uranium mining site on the stream sediments (Crucea mine, Romania). Scientific Annals, School of Geology, Aristotle University of Thessaloniki. Proceedings of the XIX CBGA Congress, Thessaloniki, Greece 100: 121–126

Pinto MMSC, Silva MMVG, Neiva AMR (2004) Pollution of water and stream sediments associated with the vale de abrutiga uranium mine, Central Portugal. Mine Water Environ 23:66–75. https://doi.org/10.1007/s10230-004-0041-3

Piper AM (1944) A graphic procedure in the geochemical interpretation of water analyses. Am Geophys Union Trans 25:914–928

Raeva D, Slavov T, Stoyanova D, Zivčič L, Tkalec T, Rode Š (2014) Expanded nuclear power capacity in Europe, Impact of Uranium Mining and Alternatives. EJOLT Report, Nº.12: 129

Rapp JS, Short WO (1981) Geology and uranium favorability of the Sonora Pass region, Alpine and Tuolumne Counties. U.S. Department of Energy, California. Report GJBX-132 (81): 145

Rios-Arana JV, Walsh EJ, Gardea-Torresdey JL (2003) Assessment of arsenic and heavy metal concentrations in water and sediment of the Rio Grande at El Paso-Juarez metroplex region. Environ Int 29:957–971

Schmitt JM, Thiry M (1987) Uranium behaviour in a Gossan-Type weathering system: example of the bertholène deposit (Aveyron, France). http://inis.iaea.org/Search/search.aspx?orig_q=RN:18085068

Sen IS, Peucker-Ehrenbrink S (2012) Anthropogenic disturbance of element cycles at the earth´s surface. Environ Sci Technol 46(16):8601–8609. https://doi.org/10.1021/es301261x

Shang J, Liu C, Wang Z, Zachara JM (2011) Effect of grain size on uranium(VI) surface complexation kinetics and adsorption additivity. Environ Sci Technol 45(14):6025–6031. https://doi.org/10.1021/es200920k

Sharma RK, Putirka KD, Stone JJ (2016) Stream sediment geochemistry of the upper Cheyenne River watershed within the abandoned uranium mining region of the southern Black Hills, South Dakota, USA. Environ Earth Sci 75:823

Silva RJ, Nitsche H (1995) Actinide environmental chemistry. Radiochim Acta 70–71(s1):377–396. https://doi.org/10.1524/ract.1995.7071.s1.377

Singh KP, Mohan D, Singh VK, Malik A (2005) Studies on distribution and fractionation of heavy metals in Gomti river sediments—a tributary of the Ganges, India. J Hydrol 312(1–4):14–27. https://doi.org/10.1016/j.jhydrol.2005.01.021

SNIRH (2018) Sistema Nacional de Informação de Recursos Hídricos. https://snirh.apambiente.pt/

Stewart DB, Mayes MA, Fendorf S (2010) Impact of uranyl-calcium-carbonato complexes on uranium (VI) adsorption to synthetic and natural sediments. Environ Sci Technol 44:928–934

Tabatabai MA (1996) Soil organic matter testing: An overview. p. 1–10. In: F. Magdoff et al. (eds). Soil Organic Matter: Analysis and Interpretation. SSSA Spec. Pub. 46. Am. Soc. Agron. Madison, WI

Takeno N (2005) Atlas of Eh-pH diagrams. Intercomparison of thermodynamic databases. Geol. Surv. Japan, Open File Rep., nº 419: 258

Tansel B, Rafiuddin S (2016) Heavy metal content in relation to particle size and organic content of surficial sediments in Miami River and transport potential. Int J Sediment Res 31(4):324–329. https://doi.org/10.1016/j.ijsrc.2016.05.004

Teixeira C, Medeiros AC, Pilar L, Lopes JT, Rocha AT (1959) Notícia explicativa da folha 18-B, Almeida. Carta geológica de Portugal na escala 1/50.000. Direcção-Geral de Minas e Serviços Geológicos. Serviços Geológicos de Portugal

Teixeira C, Medeiros AC, Pilar L, Carvalhosa A, Ferro MN, Rocha AT (1962) Notícia explicativa da folha 18-A, Vila Franca das Naves. Carta geológica de Portugal na escala 1/50.000. Direcção-Geral de Minas e Serviços Geológicos. Serviços Geológicos de Portugal

Tessier A, Campbell PGC (1987) Partitioning of trace metals in sediments: relationships with bioavailability. Hydrobiologia 149(1987):43–52

Thomas GW (1982) Exchangeable cations. In: Page, A.L. (Ed.). Methods of Soil Analysis, Part 2, Second Edition. Agronomy, Madison, W1: 9

Tserenpil Sh, Maslov OD, Norov N, Liu QC, Fillipov MF, Theng Benny KG, Belov AG (2013) Chemical and mineralogical composition of the Mongolian rural soils and their uranium sorption behavior. J Environ Radioactiv 118:105–112

USEPA (2005) Partition coefficients for metals in surface water, soil, and waste. Ecosystems Research Division National Exposure Research Laboratory 960 College Station Road Athens, GA 30605. EPA/600/R-05/074.

Wang X, Li Y (2011) Measurement of Cu and Zn adsorption onto surficial sediment components: New evidence for less importance of clay minerals. J Hazard Mater 189(3):719–723. https://doi.org/10.1016/j.jhazmat.2011.03.045

Wang J, Liu J, Li H, Chen Y, Xiao T, Song G, Chen D, Wang C (2017) Uranium and thorium leachability in contaminated stream sediments from a uranium minesite. J Geochem Expl 176:85–90. https://doi.org/10.1016/j.gexplo.2016.01.008

Wang Q, Chen QY, Yan D, Xin SG (2018) Distribution, ecological risk, and source analysis of heavy metals in sediments of Taizihe River. China Environ Earth Sci 77(16):569–583. https://doi.org/10.1007/s12665-019-8080-z

WHO (2017) Guidelines for drinking - water quality: fourth edition incorporating the first addendum, Geneva: World Health Organization, 2017, License: CC BY-NC-SA 3.0 IGO. Available at http://whqlibdsc.who.int/publications/2017/978924154851_eng.pdf.

Wilkinson L, Friendly M (2009) The history of the cluster heat map. Am Stat 63(2):179–184. https://doi.org/10.1198/tas.2009.0033

Williamson JE, Carter JM (2001) Water-Quality Characteristics in the Black Hills Area, South Dakota. U.S. Department of the Interior. U.S. Geological Survey Water-Resources Investigations Report 01–4194

World Nuclear Association (2015) Supply of Uranium. Available from: http://www.world-nuclear.org/info/inf75.html. Accessed 02 May 2019

Xie Y, Lu G, Yang C, Qu L, Chen M, Guo C et al (2018) Mineralogical characteristics of sediments and heavy metal mobilization along a river watershed affected by acid mine drainage. PLoS ONE 13(1):e0190010. https://doi.org/10.1371/journal.pone.0190010

Yan CZ, Li QZ, Zhang X, Li GX (2010) Mobility and ecological risk assessment of heavy metals in surface sediments of Xiamen Bay and its adjacent areas. China Environ Earth Sci 60(7):1469–1479. https://doi.org/10.1007/s12665-009-0282-3

Yi L, Gao B, Liu H, Zhang Y, Du C, Li Y (2020) Characteristics and assessment of toxic metal contamination in surface water and sediments near a uranium mining area. Int J Environ Res Public Health 17(2):548. https://doi.org/10.3390/ijerph17020548

Yusan S, Erenturk S (2011) Sorption behaviors of uranium(VI) ions on α-FeOOH. Desalin 269:58–66

Zheng L, Zhongkui Z, Miaomiao R, Zhanxue S (2020) Assessment of heavy metals and arsenic pollution in surface sediments from rivers around a uranium mining area in East China. Environ Geochem Health 42:1401–1413. https://doi.org/10.1007/s10653-019-00428-x

Zielinski RA, Otton JK, Schumann RR, Wirt L (2008) Uranium in surface waters and sediments affected by historical mining in the Denver west 1:100.000 quadrangle, Colorado, U.S. Geol. Surv. Scien. Invest. Report, 2007, 5: 246.